



1 **Composition and sources of carbonaceous aerosol in the European Arctic at Zeppelin**
2 **Observatory, Svalbard**

3
4 Karl Espen Yttri^{1*}, Are Bäcklund¹, Franz Conen², Sabine Eckhardt¹, Nikolaos Evangeliou¹, Markus
5 Fiebig¹, Anne Kasper-Giebl³, Avram Gold⁴, Hans Gundersen¹, Cathrine Lund Myhre¹, Stephen Matthew
6 Platt¹, David Simpson^{5,6}, Jason D. Surratt^{4,7}, Sönke Szidat⁸, Martin Rauber⁸, Kjetil Tørseth¹, Martin
7 Album Ytre-Eide¹, Zhenfa Zhang⁴ and Wenche Aas¹

8
9 ¹NILU - Norwegian Institute for Air Research, P.O. Box 100, N-2027 Kjeller, Norway

10 ²Department of Environmental Sciences, University of Basel, Basel, Switzerland

11 ³TU Wien, Institute of Chemical Technologies and Analytics, 1060 Vienna, Austria

12 ⁴Department of Environmental Sciences and Engineering, Gillings School of Global Public Health,
13 University of North Carolina at Chapel Hill, Chapel Hill, NC 27599, USA

14 ⁵EMEP MSC-W, Norwegian Meteorological Institute, Oslo, Norway

15 ⁶Department of Earth & Space Sciences, Chalmers Univ. Technology, Gothenburg, Sweden

16 ⁷Department of Chemistry, College of Arts and Sciences, University of North Carolina at Chapel Hill,
17 Chapel Hill, NC 27599, USA

18 ⁸Department of Chemistry, Biochemistry and Pharmaceutical Sciences & Oeschger Centre for Climate
19 Change Research, University of Bern, 3012 Bern, Switzerland

20
21 *To whom correspondence should be addressed: E-mail address: key@nilu.no

22
23
24
25
26
27
28
29
30
31
32
33
34
35
36
37
38
39
40
41



42 **Abstract**

43 Our current understanding of Arctic carbonaceous aerosol (CA) is rudimentary and there is a lack of
44 long-term observations for many components, such as organic aerosol (OA), exceptions to this include
45 equivalent black carbon (eBC) and methane sulfonic acid (MSA).

46 To address this, we analyzed long-term measurements of organic carbon (OC), elemental carbon
47 (EC), and source-specific organic tracers from 2017 to 2020 to constrain CA sources in the rapidly
48 changing Arctic. We also used absorption photometer (aethalometer) measurements to constrain
49 equivalent BC from biomass burning (eBC_{BB}) and fossil fuel combustion (eBC_{FF}) using Positive Matrix
50 Factorization (PMF).

51 Our analysis showed that organic tracers are essential to understand Arctic CA sources. For
52 2017 to 2020, levoglucosan had a bimodal seasonality, with a signal from residential wood combustion
53 (RWC) in the heating season (H-season; November to May) and from wildfires (WF) in the non-heating
54 season (NH-season; June to October), demonstrating a pronounced inter-annual variability in the WF
55 influence. Biogenic secondary organic aerosol (BSOA) species (2-methyltetrols) from isoprene
56 oxidation appeared only in the NH-season, peaking in July to August. Intrusions of warm air masses
57 from Siberia in summer caused three- and ninefold increases in 2-methyltetrols compared to 2017 to
58 2018, in 2019 and 2020, respectively, warranting investigation of the local vs. the long-range
59 atmospheric transport (LRT) contribution, as certain Arctic vegetation has highly temperature sensitive
60 biogenic volatile organic compounds (BVOC) emission rates. Primary biological aerosol particles
61 (PBAP) tracers (various sugars and sugar-alcohols) were elevated in the NH-season but evolved
62 differently, whereas cellulose was completely decoupled from the other PBAP tracers. Peak levels of
63 most PBAP tracers and of 2-methyltetrols were associated with WF emissions, demonstrating the
64 importance of measuring a broad spectrum of source specific tracers to understand sources and dynamics
65 of CA. Finally, CA seasonality is heavily influenced by long-range atmospheric transport (LRT)
66 episodes, since background levels are extremely low. E.g., we find the OA peak in the NH-season is as
67 strongly influenced by LRT as is EC during Arctic Haze (AH).

68 Source apportionment of CA by Latin Hypercube Sampling (LHS) showed a mixed contribution
69 from RWC (46%), fossil fuel (FF) sources (27%), and BSOA (25%) in the H-season, whereas BSOA
70 (56%) prevailed over WF (26%) and FF (15%) in the NH-season. Source apportionment of eBC by PMF
71 showed that FF combustion dominated eBC ($70 \pm 2.7\%$), whereas RWC ($22 \pm 2.7\%$) was more abundant
72 than WF ($8.0 \pm 2.9\%$). Modeled BC concentrations from FLEXPART attributed an almost equal share
73 to FF ($51 \pm 3.1\%$) and BB. Both FLEXPART and the PMF analysis concluded that RWC is a more
74 important source than WF. However, with a modeled RWC of $30 \pm 4.1\%$ and WF of $19 \pm 2.8\%$,
75 FLEXPART suggests relatively higher contributions to eBC from these sources.

76 We find that OA ($281 \pm 106 \text{ ng m}^{-3}$) is a significant fraction of the Arctic PM₁₀ aerosol particle mass,
77 though less than sea salt aerosol (SSA) ($682 \pm 46.9 \text{ ng m}^{-3}$) and mineral dust (MD) ($613 \pm 368 \text{ ng m}^{-3}$)
78 as well as typically non-sea-salt sulfate (nssSO₄²⁻) ($314 \pm 62.6 \text{ ng m}^{-3}$), originating mainly from



79 anthropogenic sources in winter and from natural sources in summer. FF combustion was the prevailing
80 source of eBC, whereas RWC made a larger contribution to eBC_{BB} than WF.

81

82 **1 Introduction**

83 The arctic is warming significantly faster than the rest of the planet due to Arctic amplification (Serreze
84 and Barry, 2011; Schmale et al., 2021). These rapid changes affect atmospheric transport and removal
85 of Arctic aerosols (Jiao and Flanner, 2016), aerosol relative source contributions (Heslin-Rees et al.,
86 2020), vegetation, and the carbon cycle.

87 Long-range atmospheric transport (LRT) of air masses from lower latitudes is an important
88 driver of the Arctic aerosol burden since local emissions are relatively much lower (e.g., Quinn et al.,
89 2007). However, the importance of LRT may be decreasing since low latitude anthropogenic aerosol
90 emissions are declining (Coen et al., 2020), while high latitude sources are increasing in importance.
91 These include, for example, increased wildfires (WF) (McCarty et al., 2020), sea salt aerosol (SSA)
92 (Heslin-Rees et al., 2020), aeolian mineral dust (MD) following glacial retreat (Zwaafink et al., 2016),
93 primary biological aerosol particles (PBAP) due to thawing permafrost and Arctic greening (Myers-
94 Smith et al., 2020), which is also likely increasing biogenic volatile organic compound (BVOC)
95 emission rates and hence biogenic secondary organic aerosol (BSOA) (Hallquist et al., 2009; Ng et al.,
96 2017; Mc Figgans et al., 2019). These changes in sources are also changing Arctic aerosol physical-
97 chemical properties and hence their climate impact. PBAP are efficient ice nucleating particles (INP) at
98 high temperatures (Tobo et al., 2019), while BSOA might act as cloud condensation nuclei (CCN) or
99 influence CCN activity (Riipinen et al., 2011), and have negative feedbacks to the Arctic climate
100 (Paasonen et al., 2013). Knowledge regarding concentration, activation temperature, composition,
101 sources, origin, and seasonality of Arctic INP and CCN is rudimentary (Creamean et al., 2018; 2019;
102 2020; Hartmann et al., 2019; 2020). The aerosol indirect effect is particularly important in the Arctic, as
103 mixed phase clouds have a long lifetime, possibly due to a lack of INP (Solomon et al., 2018), thus
104 changes in INP are deemed more important than CCN regarding Arctic cloud radiative properties
105 (Solomon et al., 2018).

106 Overall, elucidating developments in local aerosol emissions and or formation, changes in LRT
107 of aerosols, and, in turn the aerosol chemical profile, is crucial to understanding a changing Arctic and
108 its regional and global climate impact. Meanwhile, understanding and validating these changes in
109 atmospheric composition requires high quality, long-term observations, which are particularly lacking
110 for carbonaceous aerosol (CA), excepting black carbon (BC), a focus of attention due to its direct climate
111 and albedo (Clarke and Noone, 1985; Pueschel and Kinne, 1995; Hansen and Nazarenko, 2004;
112 Eleftheriadis et al. 2009; Hirdmann et al., 2010). A second exception is methane sulfonic acid (MSA)
113 with time series from 1977 at Alert (Sharma et al., 2019) and 1980 at Barrow (Quinn et al., 2009), though
114 its role in aerosol formation, growth, and radiative forcing is still a matter of ongoing research (Hodshire
115 et al., 2019).



116 Significant contributions to Organic matter (OM) of Eurasian origin to Arctic Haze (AH) have
117 been suggested since the 1970s (Quinn et al., 2007), quantified mostly only as a residual fraction (Quinn
118 et al., 2002) and from measurements of selected organic species (Li et al., 1993). Even short-term, direct,
119 measurements of organic carbon (OC) or OM are scarce (e.g., Hansen et al., 2014; Barrett et al., 2015;
120 Ferrero et al., 2019) and not suited to establish seasonality, annual mean, or inter annual variability. The
121 nearly two-year long study of Ricard et al. (2002) at Sevetjärvi (Finland) is one of three exceptions,
122 though at a latitude of $< 70^\circ$ N, and hence not representative of the high Arctic, with e.g., lower AH and
123 more BVOCs in summer. Meanwhile, Barret et al. (2017) report 1 year of OC data at Barrow, and
124 Moschos et al. (2022) present the most comprehensive study on Arctic OA to this date (up to 3 years of
125 data from 8 Arctic sites).

126 OC levels are not useful in elucidating sources per se, and supporting information is generally
127 needed. For example, elemental carbon (EC) (or equivalent black carbon eBC) demonstrates the
128 presence of OC from fossil fuels (FF) combustion and biomass burning (BB), essential to source
129 apportionment efforts and monitoring of the otherwise unperturbed Arctic atmosphere. Winiger et al.
130 (2019), attributed $25 \pm 16\%$ of EC to BB in winter and $42 \pm 19\%$ in summer via radiocarbon (^{14}C)
131 analysis. Further separation of BB into residential wood combustion (RWC), WF and agricultural waste
132 burning (AWB) requires inclusion of satellite observations such as MODIS (Moderate Resolution
133 Imaging Spectroradiometer) (Giglio et al., 2003), and transport modelling (Stohl et al., 2006), although
134 seasonality can be a useful qualifier. Stohl et al. (2013) point to gas and oil industry flaring as a major
135 source, contributing 42% to Arctic annual mean BC surface concentrations. ^{14}C analysis by Barrett et
136 al. (2017) shows that contemporary OC from biogenic emissions dominates in summer, while
137 contemporary and fossil OC levels are approximately equal in winter. Moschos et al. (2022) applied
138 positive matrix factorization (PMF) to spectral data of water-soluble organic carbon extracts (offline
139 analysis using an aerosol mass spectrometer, AMS), finding three anthropogenic dominated factors:
140 oxygenated organic Aerosol (OOA), Arctic Haze (AH); and primary organic aerosol (POA)), and three
141 from natural-dominated emissions: methane sulfonic acid-related organic aerosol (MSA-OA), primary
142 biological organic aerosol (PBOA), biogenic secondary organic aerosol (BSOA)), prevailing in winter
143 and in summer, respectively, with equally large contributions.

144 Source specific organic tracers measured in the Arctic, include levoglucosan for BB (e.g.,
145 Schneidmesser et al., 2009; Fu et al., 2013; Zangrando et al., 2013; Hu et al., 2013a; Yttri et al., 2014;
146 Feltracco et al., 2020), sugars and sugar-alcohols for PBAP (e.g., Fu et al., 2009b; Fu et al., 2013;
147 Feltracco et al., 2020), and different oxidation products of isoprene (e.g., 2-methyltetrols), monoterpenes
148 (e.g., 3-Methyl-1,2,3-butane-tricarboxylic acid) and sesquiterpenes (e.g., β -caryophyllinic acid), for
149 BSOA (Fu et al., 2009a; Fu et al., 2013; Hu et al., 2013). Most of these studies were for short time
150 periods, or a part of the year, largely failing to address seasonal, annual and interannual variability of
151 sources and their impact on the Arctic CA, excepting the one-year study of Yttri et al. (2014), and the
152 multi-seasonal study of Feltracco et al. (2020).



153 Lack of long-term OA measurements limits knowledge of Arctic aerosol mass closure. Further,
154 OA speciation, needed for source attribution and for studying its impact on CCN and INP is scarce.
155 Here, we present four years of OC and EC, organic tracer, and eBC_{BB} and eBC_{FF} measurements made
156 at the high Arctic Zeppelin Observatory (Ny-Ålesund, Svalbard), providing multiyear insights to Arctic
157 CA and the fundamental knowledge needed to understand changes in Arctic CCN and INP and hence
158 the impact of a changing Arctic on regional and global climate.

159

160 **2 Experimental**

161 **2.1 Sampling site**

162 The Zeppelin Observatory (78°5' N 11°5' E, 472 m above sea level, asl) is located on the Zeppelin
163 Mountain on the 20 km long and 10 km wide Brøgger peninsula, 2 km south of the remote Ny-Ålesund
164 settlement on the west coast of the Spitsbergen Island in the Svalbard archipelago (Norway, Fig. 1; Platt
165 et al., 2022). The 26 km long Kongsfjorden to the northeast and the 88 km long Forland straight in the
166 west, surround the peninsula. The Observatory lies in the northern Arctic tundra zone, surrounded by
167 barren ground largely consisting of bare stones, and occasionally a thin layer of topsoil with scarce
168 ground vegetation, mostly growing on plains at lower altitudes, and snowpacks, and glaciers. There is
169 very little influence of emissions from the Ny-Ålesund settlement, as the Observatory is typically above
170 the boundary layer.

171 The Svalbard climate reflects its high Northern latitude, but is moderated by the North Atlantic
172 Current, with substantially higher temperatures than at corresponding latitudes in continental Russia and
173 Canada, particularly in winter. Hence, the Kongsfjorden basin is considered relatively verdant due to its
174 favorable micro-climate, and ~180 plant species, 380 mosses, and 600 lichens are registered on the
175 Svalbard Archipelago (Vegetation in Svalbard, 2023). However, a short growing season (June to
176 August), 4 months of polar night, and 8 to 9 months of snow (Fig. 2) do not provide optimal conditions
177 for growth (Karlsen et al., 2014). Annual precipitation at Western Svalbard is around 400 mm.

178 The Zeppelin Observatory is part of many networks including the European Evaluation and
179 Monitoring Program (EMEP, www.emep.int), the Global Atmospheric Watch (GAW,
180 <https://public.wmo.int/en/programmes>), the Arctic Monitoring and Assessment Program (AMAP,
181 www.amap.no), and is included in the EU infrastructure ACTRIS (Aerosols, Clouds and Trace gases
182 Research InfraStructure Network, www.actris.eu)

183

184 **2.2 Sampling, handling, and storage of ambient aerosol filter samples**

185 We used a Digital high-volume sampler (PM₁₀ inlet, flow rate 666 L min⁻¹, filter face velocity 72.1 cm
186 s⁻¹) to obtain ambient aerosol filter samples. We placed the sampling inlet 2 m above the Observatory
187 roof and 7 m above ground level. We collected aerosol particles on pre-fired (850 °C; 3 h) quartz fiber
188 filters (PALLFLEX Tissuequartz 2500QAT-UP; 150 mm in diameter) for one week. We used a quartz
189 fiber filter behind quartz fiber filter (QBQ) set up to estimate the positive sampling artifact of OC



190 (McDow and Huntzicker, 1990). We shipped the filters in their respective filter holders, wrapped in
191 baked aluminum foil, and placed them in double zip lock bags. Before exposure and analysis, we stored
192 the samples in a freezer (-18°C). For each 1.5 month of sampling, we assigned one field blank, which
193 was treated in the same manner regarding preparation, handling, transport, and storage as the exposed
194 filters, except that they were not inserted in the sampler.

195 We collected the aerosol filter samples from 5 January 2017 to 4 January 2021 as part of the
196 Norwegian national monitoring programme (Aas et al., 2020)

197

198 **2.3 Measurement of OC and EC**

199 We performed Thermal-optical analysis (TOA) using the Sunset Lab OC/EC Aerosol Analyzer. We
200 used transmission for charring correction and operated the instrument according to the EUSAAR-2
201 temperature program (Cavalli et al., 2010). As part of the joint EMEP/ACTRIS quality assurance and
202 quality control effort, we regularly intercompared the performance of the OC/EC instrument (e.g.,
203 Cavalli et al., 2016).

204

205 **2.4 Measurement of organic tracers**

206 **2.4.1 Monosaccharide anhydrides, 2-methyltetrols, sugars, and sugar-alcohols**

207 We determined concentrations of monosaccharide anhydrides, sugar-alcohols, 2-methyltetrols,
208 monomeric and dimeric sugars in PM₁₀ filter samples using ultra-performance liquid chromatography
209 (UPLC) (Vanquish UPLC, Thermo) in combination with Orbitrap Q-Exactive Plus (Thermo Fischer
210 Scientific) operated in the negative electrospray ionization (ESI) mode: resolution 70 000 FWHM (full
211 width at half maximum) at 200 Dalton.

212 We added isotopically labelled internal standard to filter punches ($2 \times 1.5 \text{ cm}^2$), which were
213 submerged in precleaned tetrahydrofuran (THF) (2 mL) in separate screw neck amber glass vials, which
214 we subjected to ultrasonic extraction (30 min). We transferred the solute to a centrifuge tube using
215 pipetting and repeated this step twice. Afterward, we evaporated the solute to 0.4 mL, spun it (10 min;
216 2000 rpm), transferred and evaporated it to dryness in a screw neck amber glass vial. The sample volume
217 was redissolved in 0.25 mL precleaned THF/Milli-Q water (55:45) and whirlmixed before analysis. The
218 extraction procedure was equal to Dye and Yttri (2005). We used two columns in series for separation
219 (two 3.0 mm \times 150 mm HSS T3, 1.8 μm , Waters Inc.), using isocratic elution (Milli-Q; 18.2 M Ω),
220 flushing with acetonitrile (High purity) at the end of the run. The Milli-Q water was purified using and
221 EDS-Pak Polisher, containing activated coal (Merck, Darmstadt, Germany), and a LC-Pak cartridge
222 (Merck, Darmstadt, Germany) containing reversed-phase silica.

223 We identified all species based on retention time and mass spectra of authentic standards, using
224 isotope-labelled standards of levoglucosan, galactosan, mannitol, arabitol, trehalose and glucose as
225 recovery standards (Table S1 in Yttri et al., 2021). The limit of detection (LOD) was 1 to 3 pg m⁻³ for
226 the monosaccharide anhydrides, 1 pg m⁻³ for the 2-methyltetrols, 4 pg m⁻³ for the sugar-alcohols, 6 pg



227 m^{-3} for the dimeric sugars and 8 pg m^{-3} for the monomeric sugars.

228

229 **2.4.2 Measurement of cellulose**

230 We based the analysis of free cellulose on the saccharification of cellulose and subsequently quantified
231 the glucose produced, following the method by Kunit and Puxbaum (1996). We switched the final
232 detection of glucose from a photometric method to HPAEC PAD (high-performance anion-exchange
233 chromatography with pulsed amperometric detection), similar to Qi et al., 2020). We extracted filter
234 aliquots with a citrate buffer (0.05 M citric acid) adjusted to pH 4 and added Thymol to a final
235 concentration of 0.05% to prevent bacterial growth. We enhanced extraction by ultrasonic agitation. We
236 added enzymes (Trichoderma reesei cellulase; Aspergillus Niger cellobiase), which had been precleaned
237 by ultrafiltration to reduce glucose blanks, for saccharification. We stopped saccharification (at $45 \text{ }^{\circ}\text{C}$)
238 after 24 h by heating the samples to $80 \text{ }^{\circ}\text{C}$. We analyzed glucose on a Dionex ICS 3000 equipped with
239 a CarboPac MA1 column, using a sodium hydroxide gradient reaching from 480 mM NaOH to 630 mM.
240 We corrected results with the free glucose contained in the samples.

241

242 **2.5 Radiocarbon measurements**

243 We conducted ^{14}C -measurements of TC and EC by complete combustion of the untreated quartz fiber
244 filter and after removal of OC, respectively, using thermal-optical analysis ($760 \text{ }^{\circ}\text{C}$, pure O_2) coupled
245 with on-line measurement in an accelerator mass spectrometer (Agrios et al., 2015). For a detailed
246 description of the analytical method and data processing, see Rauber et al. (2023).

247

248 **2.5.1 Selection criteria for samples subject to radiocarbon analysis**

249 We picked a filter sample for each month of the year from samples collected from 2017 to 2018 to
250 capture the seasonal variability in source composition, resulting in a data capture range of 20% in
251 February to 67% in September. We pooled two consecutive samples for the months of June, July,
252 August, September, October, and December to meet the LOD ($3 \text{ } \mu\text{g C}$) for EC. Moreover, we aimed for
253 the front/back filter carbon content ratio >3 , but this criterion was not met for one of the samples in
254 June, September, October, and for two samples in December.

255 We analyzed ^{14}C -TC on both front and back filters, while ^{14}C -EC was analyzed only on front
256 filters. To measure ^{14}C -EC, we used three circular punches (22 mm diameter) from the filter sample
257 aliquot (16.6 cm^2). We used the remaining front filter area (5.2 cm^2) for ^{14}C -TC analysis, along with an
258 equivalent area of the back filter.

259

260 **2.6 Measurement of the aerosol absorption coefficient by multi wavelength Aethalometer**

261 We obtained measurements of aerosol absorption coefficient (Babs) using a 7-wavelength (370, 470,
262 520, 590, 660, 880, and 950 nm) absorption photometer (AE33 Aethalometer, Magee Scientific)
263 downstream of a PM_{10} inlet, yielding equivalent black carbon (eBC) by normalization with the mass



264 absorption cross section (MAC) via co-located EC measurements. We determined two eBC categories
265 using a novel application of positive matrix factorization (PMF) (Yttri et al., 2021; Platt et al., in prep.).
266 These categories were based on the Aerosol Ångström Exponent (AAE), with one having a low AAE
267 (~1), resulting from efficient combustion of mainly liquid fossil fuel, denoted eBC_{FF}, and the other
268 having a high AAE (~1.6), mainly associated with biomass burning (eBC_{BB}) and possibly residential
269 coal combustion.

270

271 2.7 Auxiliary data

272 We downloaded concentrations of SO₄²⁻, Cl⁻, Na⁺, K⁺, Mg²⁺, Ca²⁺, Al, Fe, Mn, and Ti from the EBAS
273 data repository (<https://ebas-data.nilu.no>). We calculated sea salt (ss) aerosol (SSA) according to
274 equations 1 – 5, and MD according to equations 6 and 7. We assumed Al, Fe, Mn, and Ti to be associated
275 exclusively with MD and present as Al₂O₃, Fe₂O₃, MnO, and TiO₂ (Alastuey et al., 2016). Si data was
276 not available and thus estimated based on an empirical factor (eq. 7), assumed present as SiO₂.

277

$$278 \text{[SSA]} = \text{[Na}^+] + \text{[Cl}^-] + \text{[ssK}^+] + \text{[ssMg}^{2+}] + \text{[ssCa}^{2+}] + \text{[ssSO}_4^{2-}] \quad (\text{eq. 1})$$

279

$$280 \text{[ssK}^+] = \text{[Na}^+] \times 0.037 \quad (\text{eq. 2})$$

$$281 \text{[ssMg}^{2+}] = \text{[Na}^+] \times 0.12 \quad (\text{eq. 3})$$

$$282 \text{[ssCa}^{2+}] = \text{[Na}^+] \times 0.038 \quad (\text{eq. 4})$$

$$283 \text{[ssSO}_4^{2-}] = \text{[Na}^+] \times 0.252 \quad (\text{eq. 5})$$

284

$$285 \text{[MD]} = \text{[SiO}_2] + \text{[Al}_2\text{O}_3] + \text{[Fe}_2\text{O}_3] + \text{[MnO]} + \text{[TiO}_2] \quad (\text{eq. 6})$$

286

$$287 \text{[SiO}_2] = 2.5 \times \text{[Al}_2\text{O}_3] \quad (\text{eq. 7})$$

288

289 2.8 Source apportionment of carbonaceous aerosol by Latin Hypercube Sampling

290 We used a Latin Hypercube Sampling (LHS) approach (Gelenscer et al., 2007; Yttri et al., 2011a) for
291 source apportionment of CA, using ¹⁴C, organic tracers, and OC and EC measurements from 13 samples
292 as input. We quantified seven CA fractions: EC from combustion of biomass (EC_{bb}) and fossil fuel
293 (EC_{ff}), OC from combustion of biomass (OC_{bb}) and from fossil fuel sources (OC_{ff}), primary biological
294 aerosol particles (OC_{PBAP}), being the sum of plant debris (OC_{pbc}) and fungal spores (OC_{pbs}), and
295 secondary organic aerosol (SOA) from biogenic precursors (OC_{BSOA}). Our calculations were based on
296 similar equations and emission ratios (ER) to those presented in Yttri et al. (2011a), except that we used
297 ¹⁴C-EC to calculate OC_{BB} and EC_{BB}. We have provided updated equations and ERs in Tables S1 to S2.
298 Calculated concentrations and fractions of the CA categories are presented in Tables S3 and S4. The
299 NH-season was covered by 98 days, while the heating (H) season was covered by 54 days.

300



301 **2.9 FLEXPART modelling**

302 We calculated BC concentrations at Zeppelin using the Lagrangian particle dispersion model
303 FLEXPART version 10.4 (Pisso et al., 2019). FLEXPART released computational particles every 3 h
304 for the whole study period at the Zeppelin Observatory, which were tracked backward in time. The
305 model was driven by ERA5 (Hersbach et al., 2020) assimilated meteorological analyses from the
306 European Centre for Medium-Range Weather Forecasts (ECMWF) with 137 vertical layers, a horizontal
307 resolution of $0.5^\circ \times 0.5^\circ$, and one-hour temporal resolution. We kept the particles in the simulation for
308 30 days after release, sufficient to include most BC emissions arriving at the site, given a typical BC
309 lifetime of 1 week (Bond et al., 2013). FLEXPART simulates dry and wet deposition of gases or aerosols
310 (Grythe et al., 2017), turbulence (Cassiani et al., 2014), unresolved mesoscale motions (Stohl et al.,
311 2005), and includes a deep convection scheme (Forster et al., 2007). Footprint emission sensitivities
312 were calculated at spatial resolution of $0.5^\circ \times 0.5^\circ$. We assumed that BC has a density of 1500 kg m^{-3} ,
313 following a logarithmic size distribution with an aerodynamic mean diameter of $0.25 \mu\text{m}$ and a
314 logarithmic standard deviation of 0.3 (Long et al., 2013).

315 The footprint emission sensitivities express the probability of any release occurring in each grid-
316 cell to reach the receptor site. When coupled with gridded emissions from any emission inventory, it
317 can be converted to modelled concentration at the receptor site. To derive the contribution to receptor
318 BC from different sources, we combined each gridded emission sector (e.g., gas flaring, transportation)
319 with the footprint emission sensitivity. We used anthropogenic emissions from the latest version (v6b)
320 of the ECLIPSE (Evaluating the CLimate and Air Quality ImPacts of ShortlivEd Pollutants) dataset,
321 which is an upgraded version of the previous version 5a, as described by Klimont et al. (2017). The
322 inventory (provided with a spatial resolution of $0.5^\circ \times 0.5^\circ$, monthly) includes:

323

- 324 • Industrial combustion (IND) – emissions from industrial boilers and industrial production processes
- 325 • Energy production (ENE) – combustion processes in power plants and generators.
- 326 • Residential and commercial sector (DOM) – combustion in heating, cooking stoves, and boilers in
327 households, public, and commercial buildings.
- 328 • Waste treatment and disposal sector (WST) – emissions from waste incineration and treatment.
- 329 • Transport sector (TRA) – emissions from all land-based transport of goods, animals, and persons
330 on road networks and off-road activities.
- 331 • Emissions from shipping activities in in-land waters (SHP).
- 332 • Gas flaring (FLR) – emissions from oil and gas facilities.

333

334 WF emissions were adopted from the Global Fire Emission Dataset version 4.1 (GFEDv4.1). The
335 product combines satellite information on fire activity and vegetation productivity to estimate gridded
336 monthly burned area and fire emissions, as well as scalars that we can use to calculate higher temporal



337 resolution emissions. All data are publicly available for use in large-scale atmospheric and
338 biogeochemical modelling (van der Werf et al., 2017). Emission factors to compute BC emissions are
339 based on Akagi et al., (2011). The spatial resolution of the current version (v4) is of $0.25^\circ \times 0.25^\circ$, daily.

340 To distinguish between modelled BC_{bb} and BC_{ff} , we combined contributions to receptor
341 concentrations from (i) DOM and WF, and (ii) ENE, FLR, IND, WST, SHP and TRA, respectively.

342

343 **3 Results and discussion**

344 Monthly mean concentrations of OC, EC, and organic tracers at Zeppelin Observatory are presented in
345 Fig. 2 and Fig. 3, and annual and seasonal means in Table 1. Our study is the first presenting eBC_{BB} and
346 eBC_{FF} data (Fig. 2) derived from multiwavelength aethalometer measurements in the Arctic, and we
347 compare them with BC_{BB} and BC_{FF} data obtained from the FLEXPART model (Table 3; Fig. 4; Fig S1)
348 and with EC_{BB} and EC_{FF} data from the LHS-approach (Sect. 3.2.1) (Table 2; Table S3 to S4). CA source
349 apportionment by the LHS-approach is presented in Fig. 5 and Tables S3 to S4. We discuss our data
350 according to the periods June to October, representing the growing season and the non-heating season
351 (NH-season), and November to May covering the non-growing season and the heating season (H-
352 season). These are obviously not absolute definitions. Phenomena of high relevance to the Arctic
353 aerosol, such as Boreal WF emissions thus largely reside in the NH-season, whereas accumulation of
354 anthropogenic emissions from Eurasia in winter and spring, known as AH, is part of the H-season.
355 Comparison is made with Birkenes Observatory (Southern Norway), representative of the lowest CA
356 levels in regional background Europe (Yttri et al., 2021) (Table S6), with Ispra, a regional background
357 site in the Po Valley (Northern Italy), one of Europe's most polluted regions (Table 6S), and the
358 Trollhaugen Observatory (Antarctica) (S7).

359

360 **3.1 Elemental carbon and organic carbon**

361 The interannual variabilities of EC (34%) and OC (38%) were comparable to SO_4^{2-} (40%), which like
362 OC can be either primary or secondary, or of LRT or local origin, and originate from natural as well as
363 anthropogenic sources, and having a time series dating back to 1991 (Platt et al., 2022). The annual
364 mean concentrations ranged from 6.5 to 16.3 ng Carbon (C) m^{-3} (EC) and from 90.3 to 197 ng C m^{-3}
365 (OC), second lowest only to levels observed in Antarctica (1.9 ng EC m^{-3} ; 12.2 ng OC m^{-3}) (Table S7)
366 (Rauber et al., in prep.) Particulate OC (OC_p) had an estimated conservative concentration of 68.3 to
367 165 ng C m^{-3} after accounting for the positive sampling artifact (OC_B). CA levels were particularly high
368 in 2020, with EC and OC increased by factors of 1.6 and 1.9, respectively compared to the mean of the
369 previous three years. For SO_4^{2-} , the increase in 2020 was only 1.25.

370 The annual mean concentration of OM (281 ± 106 ng m^{-3}) was less than SSA, MD, and even
371 non-sea salt (nss) SO_4^{2-} , although not for all four years considered ($OM > nss SO_4^{2-}$ for 2020) (Table 2).

372 Elevated EC concentration in the H-season correspond with the AH phenomenon (Shaw, 1995),
373 and is consistent to that previously shown for eBC (Eleftheriadis et al., 2009) and SO_4^{2-} (Quinn et al.,



374 2007; Platt et al., 2022). However, three of the four highest weekly EC concentrations occurred in the
375 NH-season (Sect. 3.5). The mean EC concentration in NH-season was five times lower than at the
376 Birkenes Observatory, and close to two orders of magnitude lower than Ispra. EC dropped by a factor
377 of two during the H-season compared to the NH-season, due to more efficient transport of air masses to
378 the Arctic in winter (Ottar et al., 1989) and by AH accumulation in winter and spring (Shaw, 1995). The
379 EC level at Zeppelin in the NH-season was eight times lower than at Birkenes and nearly 60 times lower
380 than at Ispra.

381 OC levels at Zeppelin was seven times lower than at the Norwegian mainland both for the H-
382 and NH-seasons. In the H-season, levels at Zeppelin were more than 50 lower than in the polluted Po
383 Valley region, while slightly more than one order of magnitude lower in the NH-season.

384 OC seasonality (Fig. 2) was characterized by a dip in May and June, a transition period between
385 the elevated levels seen for the AH period and the mid-summer. Contemporaneous measurements of
386 organic tracers (BB, BSOA and PBAP), EC, eBC_{BB} and eBC_{FF}, largely explained the seasonality. EC
387 was elevated throughout the AH period, pointing to a dominant contribution of OC from combustion of
388 FF and BB, whereas BSOA and PBAP tracers (except for cellulose) did not start increasing until June.
389 Note that Fu et al. (2009a) found terpene oxidation products, such as 3-Methyl-1,2,3-butane-
390 tricarboxylic acid (3-MBTCA) to be elevated compared to most isoprene oxidation products during the
391 AH period at Alert (Canadian Arctic), and that only isoprene oxidation products were measured in the
392 present study. Further, results presented in section 3.4.3 suggest a 25% BSOA contribution to CA even
393 in winter. The BB tracer levoglucosan decreased greatly from February to March, indicating that OC
394 from fossil sources became more important as the AH period progressed. However, we speculate that
395 there was a substantial degradation of levoglucosan from the end of the polar night (15 February) or as
396 day length became significant, as eBC_{BB} persisted until the end of the AH period in April, as seen for
397 eBC_{FF}. Marine MSA starts increasing in April but contributed <6% to OC for April to August 2017 to
398 2020, using monthly mean MSA data from Zeppelin for 1998 to 2004 for calculation (Sharma et al.,
399 2012). Marine heterogenic polymer-gels are likely to contribute to Arctic CA, but levels are low (Karl
400 et al., 2013), and are not addressed in this study. BB, BSOA and PBAP tracers typically peaked in July
401 and August, but whereas BSOA tracers decreased abruptly in early fall, PBAP tracers persisted to late
402 fall, whereas BB tracers, EC, eBC_{BB}, and eBC_{FF} started increasing again towards the end of the year.

403 Eight of the ten highest OC concentrations were observed in the NH-season, while for EC, seven
404 of the ten highest concentrations were observed in the H-season. Low emissions within the Arctic make
405 OC, and EC, seasonality susceptible to LRT episodes, and we find that the OC peak in the NH-season
406 is as strongly influenced by LRT as is EC during AH. We discuss three of these episodes in section 3.5.

407

408 **3.2 Biomass burning and fossil fuel combustion sources**

409 **3.2.1 Levoglucosan**

410 Annual mean levoglucosan concentrations ranged from 0.335 to 0.919 ng m⁻³, which is comparable to



411 the annual mean (0.680 ng m^{-3}) reported for Zeppelin for March 2008 to March 2009 (Yttri et al., 2014).
412 The inter annual variability was 40%, similar to major aerosol constituents such as OC and SO_4^{2-} . In
413 2020, the annual mean was twice as high as the mean of the previous three years, with an increase
414 attributed to elevated monthly means ($\sim 2 \text{ ng m}^{-3}$) in February, July, and October (Fig. 3).

415 Increased levels and peak concentrations of levoglucosan in the H-season reflected RWC
416 emissions, as shown by Yttri et al. (2014). Increased levels in July and August were not shown by Yttri
417 et al. (2014), partly due to missing data, although impact from wild and agricultural fires was predicted
418 by modelling. In the present study, increased levels in July and August were a hallmark of the
419 levoglucosan time series, pointing to the importance of WF emissions. FLEXPART model transport of
420 modelled BC emissions also showed a substantial influence of WF emissions for July and August (2017
421 to 2020) (Fig. S1). The levoglucosan concentration in the 2020 NH-season was ~ 3 -times higher than
422 the average of the three previous years, demonstrating a pronounced inter annual variability in WF
423 influence at Zeppelin. The levoglucosan to mannosan ratio (L/M) was lower for the NH-season ($4.8 \pm$
424 1.2) compared to the H-season (7.5 ± 1.9) (Fig. 3; Table S6) and might reflect a shift from WF and AWB
425 in the NH-season to RWC in the H-season. Our findings correspond with L/M ratios < 5 in summer at
426 Gruebadet (Ny-Ålesund) (Feltracco et al., 2020), but the very high L/M ratios (occasionally > 40) in
427 spring argued to be emissions from crops residue burning in Asia were not observed.

428

429 **3.2.2 EC_{BB} and EC_{FF} obtained from radiocarbon measurements and LHS**

430 Tracer based LHS source apportionment found that BB was the primary source of EC in all but one of
431 the 13 samples analyzed (Table S3 to S4). $61 \pm 15\%$ of EC, with the percentage varying by season: 67
432 $\pm 5\%$ in the NH-season when EC levels were low and influenced by WF, and $57 \pm 18\%$ in the H-season
433 when RWC dominates. Our results showed a much higher BB fraction in the H-season than Winiger et
434 al. (2019) for the H-season 2012 to 2013 (36 to 39%), whereas it matched that of the AH period in 2009
435 ($57 \pm 21\%$) (Winiger et al., 2015). The BB fraction in NH-season was slightly higher than the 58 to 62%
436 range for the NH-season in 2013 (Winiger et al., 2019). Notably, differences in sample preparation and
437 in ^{14}C analytical protocol should be considered along with inter annual variability, seeking an
438 explanation to the observed differences.

439 The weekly maximum BB fraction in Feb. 2017 (81%) was somewhat lower than the extremely
440 high (95 to 98%) daily BB fractions during AH at Zeppelin in 2009 (Winiger et al., 2015). Although no
441 conclusive explanation was given to the extreme values reported by Winiger et al. (2015), it cannot be
442 excluded that that BB emissions can greatly prevail for an entire week. eBC_{BB} apportioned by PMF
443 (Sect. 3.2.3), supports nearly exclusive (90%) BB contributions for 24 h (Fig. S2), but not for an entire
444 week (80%) (not shown). The weekly minimum BB fraction for Jan. 2018 (21%) was unprecedented
445 compared to Winiger et al. (2015) (39%). FLEXPART footprints for the Feb. 2017 and the Jan. 2018
446 samples were similar, covering North-West Russia and North-East Greenland (not shown), providing
447 no further insight to their extreme values, and thus “highlights the complexity of BC in the Arctic



448 atmosphere, where the generally low BC levels may be strongly influenced by point sources or
449 occasional combustion practices” (Winiger et al., 2015).

450

451 **3.2.3 eBC from biomass burning and fossil fuel combustion obtained from PMF**

452 The eBC (sum of eBC_{BB}, and eBC_{FF}) and EC time series were similar, with enhanced levels during AH,
453 a small increase in mid-summer, and a slight increase towards the end of the year. FF was the major
454 fraction of eBC annually ($70 \pm 2.7\%$), in the H-season ($71 \pm 2.7\%$), and in the NH-season ($67 \pm 6.7\%$)
455 (Table 3; Fig. 4).

456 Previous modelling studies indicate that WF is the primary source of Arctic BC during summers
457 (Stohl et al., 2013; McCarty et al., 2021). ¹⁴C-EC measurements support this for Zeppelin, but not other
458 high Arctic observatories (Table 4; Winiger et al., 2019). By the crude, but still realistic, assumption
459 that all eBC_{BB} in the NH-season comes from WF (here: eBC_{WF}), then the 27 to 42% contribution of
460 eBC_{WF} calculated for the 2017 to 2020 NH-seasons is lower than previous results. Neither eBC_{WF}, nor
461 eBC_{RWC} (eBC_{BB} in H-season), prevailed monthly (Fig. S3), although by a short margin for October 2017,
462 July 2020, and October 2020 (46 to 48%). WF was estimated to contribute 5.4 to 12% to eBC annually,
463 and RWC 20 to 26%, emphasizing RWC as a larger source of eBC than WF.

464 FLEXPART predicted an almost equal share of BC from BB and FF annually, whereas BC_{FF}
465 ($56 \pm 3.6\%$) prevailed in the H-season and BC_{BB} ($61 \pm 3.3\%$) in the NH-season (Table 3), similar to
466 results found in Stohl et al. (2013). For a direct comparison, BC_{WF} (and BC_{RWC}) was calculated similarly
467 from FLEXPART BC_{BB} output as eBC_{WF} from eBC_{BB} by PMF, i.e., BC_{WF} equals all BC_{BB} in the NH-
468 season, whereas BC_{RWC} equals all BC_{BB} in the H-season. Comparing this proxy BC_{WF} with the
469 FLEXPART modelled BC_{WF}, provided a ratio of 0.97 to 1.09 for 2017 to 2020, indicating that the BC_{WF}
470 proxy is a sound approximation. With 16 to 22% of BC attributed to WF and 27 to 36% to RWC annually
471 (Fig. 4; Table 3), FLEXPART concludes, in the same way as PMF, that RWC > WF, but suggests higher
472 percentages for WF and RWC fractions.

473 Neither PMF nor FLEXPART seem to fully reflect the predominant role of BC from WF above
474 50 °N, which McCarty et al. (2021) suggest are larger than emissions from anthropogenic residential
475 combustion, transportation, and flaring, combined. In 2020, 56% of the BC emissions North of 65 °N
476 were attributed to open biomass burning by McCarty et al. (2021), whereas 12% (PMF) and 22%
477 (FLEXPART) of (e)BC was attributed to WF at Zeppelin for 2020 in the present study. Spatial
478 variability and vertical distribution of the emissions might explain part of the discrepancy, as might mid
479 latitude emissions below 65 °N, being less influenced by WF. Vertically resolved BC concentrations in
480 the Arctic in spring and summer based on aircraft measurements show a decrease with increasing altitude
481 (Jurányi et al., 2023), but this remains yet to be confirmed for BC from WF.

482 Using the levoglucosan BB tracer, the WF fraction (36 to 64%; Table 3) was higher than seen
483 for both eBC_{WF} (17 to 35%) (PMF) and BC_{WF} (32 to 45%) (FLEXPART), contributing 64% in 2020.
484 However, degradation of levoglucosan during LRT, and lack of representative (e)BC/levoglucosan ERs



485 for a vast number of fuel categories, vegetation types, and not least combustion conditions, implies
486 considerable uncertainty in deriving the RWC/WF (e)BC split using this technique.

487 Comparing PMF results to the few samples subjected to ^{14}C measurements and source
488 apportionment by tracer based LHS showed that these two approaches were on opposite ends of the
489 scale, with FLEXPART in between (Table 4). Radiocarbon and LHS estimated a BB fraction twice as
490 high as the PMF approach, whereas it is the other way around for FF. The three methods used to
491 apportion BC all harmonized in showing a more abundant BB fraction in the NH-season than in the H-
492 season, and vice versa for FF. An explanation to the great difference in the BB/FF split derived from the
493 aethalometer and ^{14}C measurements should be explored further. Notably, BB and FF fractions of eBC
494 derived from PMF were more aligned with those from radiocarbon measurements at Zeppelin in 2012
495 to 2013 (Winiger et al., 2019) than in the present study, and with fractions derived from levoglucosan
496 measurements at Zeppelin in winter 2008 to 2009 (Yttri et al., 2014). Inter annual variability make such
497 a comparison indicative only, but differences in methodological approaches should not be excluded.

498 Nearly exclusive (90%) contributions to eBC were seen for both eBC_{BB} and eBC_{FF} for periods
499 of 24 h (Fig. S2, upper left panel). This corresponds with 24 h ^{14}C -EC data from Zeppelin dominated
500 (EC $f_{bb} > 95\%$) by contemporary carbon (Winiger et al., 2015), and ^{14}C -EC data dominated (EC $f_{ff} >$
501 95%) by fossil carbon observed at other high Arctic sites (Winiger et al., 2019). Exclusive contributions
502 were most frequent for eBC_{FF} and seen for 1.1% of the dataset compared to 0.1% for eBC_{BB}. Hence,
503 with a few exceptions, eBC_{BB} and eBC_{FF} co-appear, reflecting common source regions (See Fig. 6; Sect.
504 3.2.4).

505

506 3.2.4 Seasonal footprints for eBC_{BB} and eBC_{FF}

507 LRT from Northern Eurasia is a predominant pattern for high eBC_{BB} and eBC_{FF} (Fig. 6), as previously
508 shown for eBC (e.g., Elefteriadis et al., 2009; Hirdmann et al., 2010; Platt et al., 2022). There was a
509 negligible difference in the footprints of the two categories, except in fall when the footprint for eBC_{BB}
510 extended towards Eastern Siberia, indicating common source regions, and mixing of air masses en route.
511 Figure S2 illustrates the most likely eBC_{BB} and eBC_{FF} mixtures occurring (left panel), and how the eBC_{FF}
512 fraction increases with rising eBC levels in winter and spring and decreases in fall, and to some extent
513 in summer (right panel), the latter due to WF influence. Indeed, the three major CA episodes at Zeppelin
514 for 2017 to 2020 all occurred in summer and fall (Sect. 3.5) and had a (marginally) prevailing eBC_{BB}
515 fraction largely attributed to WF by FLEXPART. Notably, eBC_{FF} and eBC_{BB} appear well mixed and
516 almost equally abundant even for the most prominent WF episodes reaching Zeppelin.

517

518 3.3 Biogenic secondary organic aerosol - 2-methyltetrols

519 2-methyltetrols (here: sum of 2-methylerythritol and 2-methylthreitol) are primarily formed from the
520 acid-catalyzed multiphase chemistry of isoprene epoxydiols (IEPOX) (Surratt et al., 2010; Lin et al.,
521 2012; Cui et al., 2018), which are important low-NO_x oxidation products of isoprene (Paulot et al.,



522 2009), the most abundant BVOC (500 Tg C yr⁻¹) globally (Williams and Koppmann, 2007), and an
523 important source of BSOA (Hallquist et al., 2009; Noziere et al., 2015). Their low-level presence in
524 the Arctic has been demonstrated in only a few studies covering a few months (e.g., Fu et al., 2009a).
525 We discuss their level, seasonality, sources, and LRT vs. local formation over four consecutive years.

526 2-methyltetrol concentrations at Zeppelin were at the lower range of those reported in Europe
527 (Ion et al., 2005; Kourtchev et al., 2005; 2008 a,b), North-America (Cahill et al., 2006; Xia and Hopke;
528 200; Cui et al., 2018), South-America (Claeys et al., 2010) and Asia (Fu et al., 2010), and consistent
529 with levels observed at Alert in the Canadian Arctic (Fu et al., 2009a). The duration of the elevated 2-
530 methyltetrols concentrations during the peak of the inter annual cycle at Zeppelin appears quite like that
531 at the Birkenes Observatory (Southern Norway) 2300 km further south: with an onset in June and peak
532 concentrations in July and August, the time series at Zeppelin is delayed by half a month compared to
533 Birkenes, although concentrations drop by mid-October at both sites. The annual mean 2-methyltetrols
534 concentration was 3 times lower at Zeppelin compared to Birkenes in 2017 and 5 in 2018. In 2019, the
535 2-methyltetrol level at Zeppelin increased by a factor of three compared to 2017 to 2018 and in 2020 by
536 a factor of nine, and thus for 2020 the annual mean at Zeppelin (1.15 ng m⁻³) was nearly twice as high
537 as the highest annual mean seen at Birkenes (0.610 ng m⁻³ in 2018).

538 The atmospheric lifetime of isoprene is < 4 hours, whereas the lifetime of 2-methyltetrols is
539 unknown (Wennberg et al., 2018) and the amount attributed to formation from locally emitted isoprene
540 vs. LRT 2-methyltetrols remains an open question. The 2-methyltetrols level at Birkenes increase by
541 nearly a factor of 20 when leaves unfold in May (Yttri et al., 2021). Consequently, the effect of leaves
542 unfolding 0.5 to 1.5 months earlier in continental Europe (the leaves of *Betula Pubescens* unfold 2.1
543 days later pr. 100 km along a South to North transect in Europe; Rötzer and Chmielewski, 2001) does
544 not seem to have an influence, suggesting that the 2-methyltetrols level largely reflect local formation.
545 At Svalbard, there are no forests, and hardly any trees, still there is vegetation (including mosses and
546 lichens) that emit isoprene, that can have emission rates that are considerably higher than those observed
547 at Southern latitudes (Kramshøj, et al., 2016). Circumpolar land masses are situated further away from
548 Zeppelin than continental Europe from Birkenes, thus local formation of 2-methyltetrols might be
549 important also at Svalbard. Marine sources of isoprene cannot be excluded, particularly in remote marine
550 areas (Liakakou et al., 2007), although macro algae seem to favor dimethyl sulfide (DMS) formation
551 rather than isoprene in the Arctic (Dani and Loreto, 2017). Further, time series of 2-methyltetrols and
552 MSA at Zeppelin (Sharma et al., 2012) do not co-vary, suggesting a non-marine origin of 2-
553 methyltetrols.

554 The increased 2-methyltetrol level at Zeppelin in 2019 to 2020 occurred during summer. From
555 30 June to 11 of August 2020, weekly mean concentrations ranged from 5.9 to 28 ng m⁻³ for four out of
556 six weeks, being up to five times higher than the highest weekly mean at Birkenes (5.6 ng m⁻³) for 2017
557 to 2018. We recognize that levoglucosan was elevated (1.0 to 6.0 ng m⁻³) for these four weeks and that
558 air masses were influenced by WF emissions in Western Russia (Fig. 7; Sect. 3.5.1). We are left



559 speculating how WF might have augmented 2-methyltetrol levels. Isoprene emissions are enhanced by
560 increased temperature and a fire plume provides favorable conditions for BSOA formation and aerosol
561 surface area for condensation. Notably, 2-methyltetrols are semi volatile (Lopez-Hilfiker et al., 2016)
562 and at high OA loadings increased partitioning to the aerosol phase will occur. Further, transport time
563 was short (Fig. S3), which is favorable concerning potential degradation of 2-methyltetrols. Increased
564 formation from local isoprene emissions is likely, as ambient temperature at Zeppelin was
565 unprecedentedly high in this period (See Sect 3.5.1 and Fig. 7 for details). The elevated 2-methyltetrol
566 concentration (3.7 ng m^{-3}) seen for the warm period in the beginning of July 2019 was not nearly as high
567 as for July and August 2020 and levoglucosan (0.04 ng m^{-3}) was not increased.

568 2-methyltetrols (here: ng C m^{-3}) contributed up to 0.34% to OC monthly in the NH-season in
569 2019 and 0.56% in 2020, being clearly higher compared to the two previous years (0.14% and 0.23%),
570 which in turn was higher than the highest monthly means at Birkenes (0.09% and 0.12%). Compared to
571 rural central Europe (0.68% in June) (Ion et al., 2005) and Boreal Forest Finland (0.88% in the July to
572 August transition) (Kourtchev et al., 2005), the highest contributions at Zeppelin in 2020 are slightly
573 lower.

574 Multi-year time series of 2-methyltetrols are rare, particularly in areas with low NO_x -
575 concentrations (Noziere et al., 2011; Cui et al., 2019). We find that the NH-season drop in the 2-
576 methylthreitol to 2-methylerythritol ratio was much more pronounced at Birkenes (0.36 ± 0.11) than at
577 Zeppelin (0.54 ± 0.12) (Table S6). A NH-season drop is also observed the Hyytiälä Observatory (Boreal
578 Forest Finland) (Kourtchev et al., 2005). Elevated ratios were observed at Zeppelin in July (0.83) and
579 August (0.70) 2020 when influenced by WF emissions, being substantially higher compared to July –
580 August (0.45 ± 0.04) of previous years. With the exceptions mentioned, the mean ratio for the NH-
581 season at Zeppelin agrees with the upper range (0.25 to 0.58) reported by others (Claeys et al., 2010),
582 and thus, relate to the formation mechanism of 2-methyltetrols outlined by Bates et al. (2014), which
583 shows a 1:2 relationship between *cis*- β -IEPOX and *trans*- β -IEPOX, accounting for >97% of observed
584 IEPOX, and which are the precursors of 2-methylthreitol and 2-methylerythritol, respectively. Notably,
585 2-methyltetrols can also result from the degradation of IEPOX-derived organosulfates through
586 hydrolysis of tertiary ones (Darer et al., 2011), however these species were not measured in the present
587 study.

588 There are studies suggesting a biological (enzymatic) origin of 2-methyltetrols, as there is an
589 enantiomer excess of both 2-C-methyl-D-erythritol and 2-C-methyl-threitol (Noziere et al., 2011;
590 González et al., 2014; Jacobsen and Anthonsen, 2015) - If the 2-methyltetrols formation was exclusively
591 abiotic, resulting from atmospheric oxidation of isoprene (Claeys et al., 2004), there would be a racemic
592 mixture of the 2-methyltetrols - This is consistent with the known production of the 2-methylerythritol
593 D-form by plants, algae, and microorganisms (Anthonsen et al., 1976, 1980; Dittrich and Angyal, 1988;
594 Ahmed et al., 1996; Duvold et al., 1997; Sagner et al., 1998; Enomoto et al., 2004). Consequently, it can
595 be questioned if 2-methyltetrols are exclusive tracers of BSOA from atmospheric oxidation of isoprene,



596 e.g., a 30 to 67% biological contribution was calculated for May to December for the Aspveten site
597 (Sweden) (Noziere et al., 2011). Unfortunately, the analysis done in the present study does not allow for
598 a proper investigation of a potential biological contribution. Cahill et al. (2006) argued for a biological
599 source based on the correlation between 2-methyltetrol and the PBAP tracers glucose ($r^2 = 0.732$) and
600 fructose ($r^2 = 0.644$) for eleven samples. At Zeppelin, r^2 for 2-methyltetrols vs. fructose (0.951), glucose
601 (0.946) and arabitol (0.801) appears elevated in the NH-season but drops substantially ($r^2 = 0.052 -$
602 0.437) when excluding the extreme values in July and August 2020. At Birkenes, correlation was non-
603 existing ($r^2 = 0.000 - 0.025$). Source apportionment of CA by PMF at Birkenes showed that the factor
604 explaining 94% of the 2-methyltetrols explained only 6% of the PBAP tracers, and that the factor
605 explaining 89% of the PBAP tracers explained only 2.5% of the 2-methyltetrols (Yttri et al., 2021).
606 Hence, statistics do not argue for a common source of 2-methyltetrols, or a fraction of 2-methyltetrols,
607 and PBAP tracers. Further, 2-methylerythritol vs. 2-methylthreitol correlated highly both at Zeppelin (r^2
608 $= 0.971$) and at Birkenes ($r^2 = 0.889$), suggesting one dominating source (abiotic secondary formation),
609 corresponding to findings by El-Haddad et al. (2011). However, potential mechanisms by which
610 biologically formed 2-methyltetrols are released to the atmosphere are not known, thus a biological
611 contribution cannot be excluded.

612

613 **3.4 Primary biological aerosol particles**

614 The interest in PBAP has grown over the last two decades, with rising awareness of its contribution to
615 the OA budget (e.g., Wake et al. 2014; Yttri et al. 2021; Moschos et al., 2022) and as a source of warm
616 INP, deemed more important than CCN regarding Arctic cloud radiative properties (Solomon et al.,
617 2018). We address a handful of PBAP tracers, discuss their levels, seasonality, and sources, including
618 cellulose, measured in Arctic aerosol for the first time.

619

620 **3.4.1 Sugars and sugar-alcohols**

621 Annual mean concentrations of sugars and sugar-alcohols were 1 to 2 orders of magnitude lower at
622 Zeppelin compared to Birkenes, reflecting the modestly vegetated Arctic and that PBAP mainly have a
623 local origin (Samaké et al., 2019). This contrasts with the factors for 2-methyltetrols (≤ 5), which are
624 secondarily formed species with a stronger regional character but might also relate to the temperature
625 sensitive high flux of BVOC for Arctic vegetation (Kramshøj et al., 2016). Higher levels of primary
626 biological organic aerosol (PBOA) at Gruvebadet (50 m asl), one km south of Ny-Ålesund, compared
627 to the Zeppelin Observatory (472 m asl) (Moschos et al., 2022) indicate a local contribution associated
628 with the more verdant lower altitude areas. However, maximum concentrations of sugars and sugar-
629 alcohols were observed for the LRT episode 22 – 27 July 2020 (Sect. 3.5.1), explaining 24% of the
630 annual sugars and sugar-alcohols loading. We are left speculating about the LRT fraction of PBAP vs.
631 that of local origin, but LRT likely makes a larger contribution to the Arctic than for more vegetated
632 southerly biomes.



633 All species experienced a modest increase in June, coinciding with the onset of the growing
634 season, but evolved differently after that, suggesting a mixture of sources, highlighting the importance
635 of measuring a broad specter of PBAP tracers. Arabitol and mannitol were elevated throughout summer
636 before successively declining towards the end of the year, fructose and glucose started decreasing
637 immediately after the peak level in July, whereas trehalose experienced comparable levels from July to
638 November. Snow cover can be decisive for PBAP levels (Yttri et al., 2007 a, b) and probably more so
639 for the non-forested Arctic. However, our data does not explicitly demonstrate an influence of the snow
640 cover, e.g., the seasonality of trehalose (and cellulose; Sect 3.4.2).

641 The composition of sugars and sugar-alcohols at Zeppelin and Birkenes varied, reflecting
642 different biomes. Glucose was the most abundant sugar regardless of the season at Zeppelin. At
643 Birkenes, glucose dominated only in winter, while arabitol and mannitol were more prominent in
644 summer. Trehalose levels were comparable or slightly higher than arabitol and mannitol at Zeppelin but
645 lower at Birkenes. Samaké et al. (2020) showed how only a few genera of fungi and bacteria were
646 responsible for the sugar and sugar-alcohol containing PBAP in PM₁₀ filter samples at a rural site in
647 France, and that these were associated with leaves rather than soil material. This strong association
648 between sugars and sugar-alcohols and vegetation likely explain the very low levels of these PBAP
649 tracers at Zeppelin compared to Birkenes. Samaké et al. (2020) point to the fungus *Cladosporium sp.*
650 when explaining ambient aerosol levels of arabitol, mannitol and trehalose, as does Yttri et al. (2007a)
651 for Birkenes. The annual mean mannitol to arabitol ratio was comparable between Zeppelin (1.1 ± 0.2)
652 and Birkenes (Table S6), to values reported for the Nordic countries (Yttri et al., 2011b) and fungal
653 spores (Bauer et al., 2008). Mannitol and arabitol were highly correlated in the NH-season ($r^2 = 0.983$)
654 when levels were elevated, and mannitol to arabitol ratio variability minor, suggesting one common
655 source prevailing. However, four samples with a mannitol to arabitol ratio ≥ 3 in the April to May
656 transition could indicate influence from another source. Mannitol is considered the most abundant
657 naturally occurring polyol, present and produced in a wide range of living organisms (Tonon et al.,
658 2017), accounting for 25% of the dry weight of macro algae for certain parts of the year (Horn et al.,
659 2000), however, our data for Zeppelin suggest that fungal spores are decisive for arabitol and mannitol
660 present in the Arctic aerosol. Assuming all mannitol was associated with fungal spores, their carbon
661 content contributed $0.5 \pm 0.2\%$ to OC annually when applying the lower OC/mannitol ratio (5.2) of
662 Bauer et al. (2002), whereas the highest monthly mean was seen for September ($1.5 \pm 1.2\%$). The
663 contribution reached 5% for only two of the weekly samples. Using the higher OC/mannitol ratio (10.8),
664 would double these estimates.

665 Glucose is a building block of natural dimers and polymers and a ubiquitous primary molecular
666 energy source, and thus an important PBAP. Small amounts of glucose are present in RWC emissions
667 (Nolte et al., 2001) and are increased in air masses influenced by forest fire smoke (Medeiros et al.,
668 2006). Notably, nine of the ten samples highest in glucose were also highly increased with respect to
669 levoglucosan and were all collected in the NH-season (Table S8), demonstrating WF as an important



670 source of glucose brought to the Arctic by LRT. A largely similar finding was made for the other sugars
671 and sugar-alcohols. Previous studies do not seem to link fungal related sugars and sugar-alcohols
672 (arabitol, mannitol, trehalose) with WF emissions (e.g., Table 5 in Medeiros et al., 2006), nor with RWC
673 emissions, e.g., levoglucosan and sugar-alcohols end up in different factors in PMF studies (Waked et
674 al., 2014; Yttri et al., 2021). This might partly be due to lack of correlation between levoglucosan and
675 sugar-alcohols for an entire data set. Indeed, no correlations between levoglucosan and sugar-alcohols
676 ($r^2_{\text{NH-season}} < 0.423$; $r^2_{\text{H-season}} < 0.056$) were obtained considering the entire data set for Zeppelin, although
677 the data presented in Table S8 clearly demonstrates a connection between WF and sugar-alcohols.

678 We estimated a 7 – 15% contribution of PBAP to OC annually, using an OC-to-PBAP_{Tracers}
679 emission ratio (ER) of 14.6 ± 2.1 (Zwaafink et al., 2022), derived from measurements in the Boreo-
680 nemoral zone (Yttri et al., 2021), keeping in mind that such an ER would be site specific.

681

682 **3.4.2 Cellulose**

683 Cellulose was the most abundant organic tracer analyzed (annual mean concentration of $2.2 \pm 0.6 \text{ ng m}^{-3}$)
684 ³), but levels were much lower than in rural areas of continental Europe (annual mean: $16.3 - 284 \text{ ng m}^{-3}$)
685 ³) (Sánchez-Ochoa et al., 2007; Brighty et al., 2022), likely due to sparse vegetation at Svalbard. The
686 highest monthly means were seen for June followed by October, but there was no pronounced
687 seasonality for cellulose as seen for the other PBAP tracers (Sect. 3.4.1). This corresponds with findings
688 made by Sánchez-Ochoa et al. (2007) who pointed to a minor seasonality “with higher winter levels
689 than expected”, and that of Puxbaum and Tenze-Kunit (2003) who associated increased cellulose levels
690 in spring with “seed production and repulsing of other cellulose containing plant material”, and
691 “production of leaf litter” in fall. High wind speed might be a driving force for generation and
692 entrainment of cellulose containing aerosol particles that is more pronounced in winter, and particularly
693 in the harsh Arctic climate, but possibly limited by snow cover. In the recent study by Brighty et al.
694 (2022), a clear seasonality was shown with increased levels in summer and fall at French and Swiss
695 rural sites.

696 Size distribution measurement of cellulose is limited and inconclusive, with highest
697 concentrations reported both for the fine (Puxbaum and Tenze-Kunit, 2003) and the coarse mode (Yttri
698 et al., 2011a; Brighty et al., 2022). Lack of comparable seasonality between nearby sites indicates that
699 local sources prevail (Brighty et al., 2022), but with a certain fraction associated with fine aerosol, LRT
700 is a possibility. Cellulose did not correlate with other PBAP tracers or levoglucosan, corresponding to
701 the findings by Brighty et al. (2022), but this does not exclude co-emission (see Sect. 3.4.1). A minor
702 fraction (0.08%) of RWC emissions was attributed to cellulose in a combustion study by Schmidl et al.
703 (2008), but we found no strong connection between the samples highest in cellulose and levoglucosan,
704 as we did for the other PBAP tracers and levoglucosan, nor between cellulose and the other PBAP tracers
705 (Table S8). The lack of resemblance between cellulose and other PBAP tracers and BB aerosol should
706 be explored further.



707 Cellulose (here ng C m^{-3}) made a $1.0 \pm 0.3\%$ contribution to OC annually, corresponding to the
708 lower range reported for rural background sites along an east to west transect across Europe ($0.7 - 3.9\%$)
709 (Sánchez-Ochoa et al., 2007), but substantially lower compared to French ($3.2 \pm 2.4\%$) and Swiss
710 ($5.9 \pm 4.4\%$) rural background sites (Brighty et al., 2022).

711 The contribution of plant debris (here: ng C m^{-3}) was estimated from cellulose (Puxbaum and
712 Tenze Kunit, 2003; Yttri et al., 2011a,b) as a $2.0 \pm 0.6\%$ contribution to OC annually, and thus somewhat
713 higher than for fungal spores ($0.5 - 1.1\%$). On a monthly basis, 4 to 6% contributions were observed in
714 all seasons. Weekly samples ($n = 23$) with a high (5 to 12%) plant debris contribution were associated
715 with low OC levels (mean: 53 ng C m^{-3} ; 22 percentile) and elevated cellulose levels (mean: 3.1 ng m^{-3} ;
716 80 percentile) and were correlated ($r^2 = 0.707$), suggesting that plant debris drives observed OC levels
717 at low concentrations. We did not observe a similar feature for fungal spores.

718

719 **3.4.3 Source apportionment of carbonaceous aerosol by Latin Hypercube Sampling**

720 Source apportionment of CA (here: TC) by the LHS approach showed that natural sources dominated
721 in the NH-season (85%) and anthropogenic in the H-season (73%), assuming all biomass burning (BB)
722 emission originated from WF in the NH-season and from RWC in H-season (Fig. 5). Even without
723 attributing BB emissions to WF, natural sources still dominated in the NH-season (60%).

724 BSOA (56%) was the most abundant natural source in the NH-season, then WF (26%) and
725 PBAP (3.2%). Compared to previous studies (Yttri et al., 2011 a and b), we found a lower PBAP
726 fraction, which we attributed to the less vegetated Arctic environment. Note that the LHS approach
727 underestimate the PBAP fraction by only accounting for fungal spores and plant debris, apportioning a
728 part of PBAP to BSOA (Yttri et al., 2021). We increased the PBAP fraction to 11% using an OC-to-
729 $\text{PBAP}_{\text{Tracers}}$ emission ratio (ER) of 14.6 ± 2.1 (Zwaafink et al., 2022), noting that the ER was obtained
730 from measurements in the boreo-nemoral zone, and thus more representative of LRT than local PBAP
731 sources.

732 RWC (46%) was the major fraction in winter followed by FF (27%) and BSOA (25%), whereas
733 PBAP (1.4%) was negligible, even when considering the upper estimate (2.7%) obtained using the ER
734 by (Zwaafink et al., 2022). The absence of 2-methyltetrols in winter indicated that BSOA was formed
735 from oxidation of mono- and sesquiterpenes and dimethyl sulfide, which seem more abundant in the
736 Arctic winter than oxidation products of isoprene (Fu et al., 2009a; Sharma et al., 2012). Further,
737 modelling studies suggest that increased condensation may explain wintertime BSOA (Simpson et al.,
738 2007), which might be particularly relevant for the low Arctic temperatures.

739 Our source apportionment results for Zeppelin are consistent with those of rural background
740 Europe (e.g., Gelencsér et al., 2007; Genberg et al., 2011; Gilardoni et al., 2011; Yttri et al., 2011a),
741 with RWC dominating in the heating season and BSOA in summer.

742

743 **3.5 LRT episodes outside the AH period**



744 LRT episodes are decisive for CA levels and seasonality observed at Zeppelin. We analyzed in detail
745 the three episodes with the highest weekly means of OC, which also had three of the four highest weekly
746 means of EC (Figs. 6 to 8). All these episodes had air masses originating from NW Eurasia.

747

748 **3.5.1 Episode 1 (22 July to 27 July 2020) – WF, BSOA, and PBAP**

749 In transition July to August 2020, CA levels were high, with peak concentrations from 22 – 27 July
750 (2172 ng C m^{-3} for OC and $59 \text{ } \mu\text{g C m}^{-3}$ for EC). These levels were the highest in four years of
751 observations, explaining 17% of the annual OC loading, but only 6% of EC. However, levels were still
752 lower than the record high concentrations ($3.5 \text{ } \mu\text{g C m}^{-3}$ for OC and $0.24 \text{ } \mu\text{g C m}^{-3}$ for EC) observed in
753 the April to May transition 2006, caused by emissions from wild and agricultural fires in Eastern Europe
754 (Stohl et al., 2007). All tracers (except cellulose) experienced maximum values during this episode, but
755 2-methyltetrols, glucose, fructose, and arabitol were the most elevated when compared to the long-term
756 annual mean and to the enhancement seen for OC. The FLEXPART footprint clearly shows an influence
757 from WF in the Khanty-Mansi district (Western Russia) (Fig. 7), corroborating to the high levoglucosan
758 concentration (6.0 ng m^{-3}). Source apportionment by PMF attributed 55% of eBC to BB, whereas
759 FLEXPART calculated 62%, with WF (95%) as the totally dominating fraction. Flaring was the
760 prevailing fossil fuel source category according to FLEXPART, explaining 58% of BC from fossil fuel
761 sources.

762 The plume transport time from the source region to the Zeppelin Observatory was short; less
763 than 7 days for 67% of eBC observed at Zeppelin 25 to 27 of July (Fig. S3), whereas on average only
764 30% of the observed eBC reaches the Arctic station after such short time. This might have contributed
765 to the high level of 2-methyltetrols, which are indicated to have short atmospheric lifetimes (Yttri et al.,
766 2021), in addition to the arguments raised in section 3.3. Certain PBAP, such as fungal spores (Bauer et
767 al., 2002; Yttri et al., 2007a) are small enough to be transported over long distances, even between
768 continents (Prospero et al., 2005), and pyro convection might bring larger sized PBAP to altitudes that
769 enables LRT (e.g., Zwaafink et al., 2022). PBAP contributed 14% of OC, using the $\text{OC-to-PBAP}_{\text{Tracers}}$
770 ER by Zwaafink et al. (2022). A relationship between deposition of nutrient-bearing aerosol from
771 Boreal WF and phytoplankton bloom in the Polar Sea has been demonstrated (Ardyna et al., 2022),
772 emphasizing the importance of Boreal WF for the Arctic environment.

773 The high CA level coincided with a prolonged period (24 to 29 July) of high temperatures,
774 unprecedented since temperature measurements were initiated at Zeppelin (1998), caused by intrusions
775 of warm air masses from Siberia; $T > 10 \text{ } ^\circ\text{C}$ for 111 consecutive hours, mean $T = 14.5 \pm 1.5 \text{ } ^\circ\text{C}$, and
776 $T_{\text{Max}} = 18.2 \text{ } ^\circ\text{C}$. A disproportionally strong warming of the Arctic compared to the midlatitudes could
777 create an important pathway of pollution to the Arctic (Stohl et al. 2007), and as for the LRT episode in
778 spring 2006 (Stohl et al., 2007), emissions from WF at lower latitudes were essential in the deterioration
779 of Arctic air quality also in July 2020.

780



781 **3.5.2 Episode 2 (28 Sep to 6 Oct 2017) – A bit of everything**

782 Air masses with a history over south-western Russia, eastern, central, and northern Europe (including
783 Scandinavia) (Fig. 8) increased the OC (549 ng C m^{-3}) and EC (52 ng C m^{-3}) concentrations at Zeppelin
784 to levels corresponding to 13% of their annual loading. Source apportionment by the LHS suggested
785 that BSOA (57%) and BB (32%) dominated CA (Table S4). Certain PBAP tracers (arabitol, mannitol
786 and trehalose) were enhanced beyond that of OC, reflecting the seasonal peak in fungal spores, but
787 PBAP contributed only 3% to CA (Table S4). An upper estimate of 13% was obtained using the OC-to-
788 PBAP_{Tracers} ER by Zwaafink et al. (2022). PMF apportioned 47% of eBC to BB, comparing well with
789 FLEXPART (51%), (ascribing 62% of BB to WF) and LHS (58%). FLEXPART apportioned the
790 majority of BC from FF combustion to traffic (55%). The mean ambient temperature during the episode
791 was enhanced compared to the long-term mean, as seen for all three episodes described.

792

793 **3.5.3 Episode 3 (2 to 10 Oct 2020) – WF and MD**

794 This episode is discussed in detail by Zwaafink et al. (2022). Briefly, the EC level (78 ng C m^{-3}) was
795 the highest in four years of observations, whereas the OC level (818 ng C m^{-3}) was much lower than
796 observations made during the July 2020 (Sect 3.5.1) episode, explaining 19% and 16% of the annual EC
797 and OC loading, respectively (Fig. 9). Levoglucosan (5.0 ng m^{-3}) was the only organic tracer elevated
798 beyond that of OC, supporting FLEXPART calculations pointing to WF emissions in Ukraine and
799 southern Russia, as one of two major sources of air pollution for this episode. Source apportionment of
800 eBC by PMF indicated an almost equal share of eBC from BB (52%) and FF combustion (48%), as do
801 FLEXPART (BB = 57% and FF = 43%), with the majority of BB attributed to WF (72%), and traffic
802 being the major FF category (52%). Mixing with MD emissions from Central Asia en route, caused a
803 MD level of $1.9 - 2.6 \mu\text{g m}^{-3}$, likely explaining the presence of carbonate (20 ng C m^{-3} ; $100 \text{ ng CO}_3^{2-} \text{ m}^{-3}$).
804 Before entering the Arctic, the polluted air masses deteriorated the air-quality in a large part of
805 northern Europe, giving PM_{10} levels around $100 \mu\text{g m}^{-3}$, and the same aerosol particle chemical signature
806 as described for Zeppelin. These levels violate EU air quality guidelines, which have daily mean limit
807 values for PM_{10} of $50 \mu\text{g m}^{-3}$.

808

809 **4 Implications**

810 Lack of long-term OA measurements has been a limitation for understanding Arctic aerosol mass
811 closure. Further, OA speciation needed for source attribution and for studying impact on CCN and INP
812 are scarce. Our four-years study shed light on some of these topics, demonstrating that OA is a
813 significant fraction of the Arctic PM_{10} aerosol particle mass, though less than SSA and MD, as well as
814 typically nssSO_4^{2-} . LRT episodes in the NH-season dominated by natural emissions and their impact on
815 OA levels, seasonality, and composition received particular focus, showing that WF also contribute to
816 high BSOA and PBAP levels in the Arctic environment. The fraction of OA attributed to local sources
817 vs. LRT is uncertain, particularly when experiencing intrusions of warm air masses from Siberia, as



818 certain Arctic vegetation species have highly temperature sensitive BVOC emission rates. Arctic CA
819 share the same feature as CA in source regions in the mid latitudes (e.g., Gelencsér et al., 2007), i.e.,
820 natural sources, particularly BSOA, prevailing in the NH-season and anthropogenic emissions,
821 predominantly RWC, in the H-season. The nine-fold increase in 2-methyltetrols observed for 2020 could
822 be a harbinger of CA from natural sources increasing in the Arctic.

823 Observed eBC attributed to WF did not dominate high-Arctic eBC in summer, contrary to
824 previous (e.g., Stohl et al., 2013) and present (this study) modeling efforts. Neither was the predominant
825 role of BC from WF emissions at Northern latitudes stated by McCarty et al. (2021) reflected in our
826 2017 to 2020 dataset. This calls for an investigation of whether the stated increase in BC from WF
827 emissions for 2010 – 2020 at Northern latitudes (McCarty et al., 2021) is reflected at Arctic ground
828 level. Up to two decades of stored multi wavelength aethalometer data for Arctic observatories,
829 combined with the outlined PMF approach enables such a trend study. Additionally, a pan-Arctic
830 investigation is encouraged for studying the spatial variability in eBC_{BB} and eBC_{FF}, facilitated by the
831 inexpensive, high time resolution multi wavelength aethalometer measurements that are widespread
832 across the Arctic observatories (Tørseth et al., 2019). These aethalometers also have the potential to
833 improve BC emissions affecting the Arctic, e.g., via inverse modelling. Increased anthropogenic activity
834 such as shipping oil and gas exploration in the Arctic, warrants further separation of eBC from FF
835 combustion, which can be attempted using additional high time resolution data as input to our analysis.
836 This appears particularly important for the flaring source, suggested by modelling to contribute 42% to
837 the annual mean BC surface concentration in the Arctic (Stohl et al., 2013), which yet remains to be
838 confirmed by observations.

839 Our study shows a wide variability amongst different methods in apportioning BC according to
840 FF and BB, warranting further investigation for a reliable abatement of sources relevant for BC in the
841 Arctic. Still, the high time resolution observational signal of eBC from BB and FF combustion derived
842 from aethalometer measurements provide a hitherto unused tool important for assessing Arctic BC.

843 Continuation of the actual time series at Zeppelin Observatory is suited for revealing potential
844 changes in the relative source composition of Arctic CA, be it from altered transport or changes in
845 emissions. It is of special interest to monitor the frequency and magnitude of WF, how BSOA and PBAP
846 concentrations develop, and if FF emissions change from increased anthropogenic activity in the Polar
847 region.

848

849 **Data availability**

850 All data used in the present paper are open access and are available at <http://ebas.nilu.no/> (NILU,
851 2023), except radiocarbon data, which are presented in Rauber et al. (2023).

852

853 **Supplement**

854 The supplement related to this article is available online at:



855

Author contributions

856 SMP, KEY, and WA were responsible for conceptualizing the study. KEY wrote the original draft of
857 the paper. WAA, SE, and KEY produced the figures. AB was responsible for collection of aerosol filter
858 samples. HG analysed the organic tracers, MR and SS did the radiocarbon measurements, and AK-G
859 was responsible for the cellulose analysis. MF, KEY, CLM, and WA carried out data curation. NE and
860 SE did the FLEXPART modelling, whereas DS and MAY did the LHS calculations. SMP and KEY
861 undertook the formal analysis. JS, AG, and ZZ acquired resources. KT, CLM and WA acquired funding.
862 All co-authors contributed to writing, reviewing, and editing the final article.
863

864

Competing interests:

866 The contact author has declared that none of the authors has any competing interests.
867

868

Acknowledgement

870

871 The Norwegian Ministry of Climate and Environment provided funding to establish the OC/EC and
872 organic tracers time series used in the present study and are gratefully acknowledged. These data are
873 reported to the EMEP monitoring programme and are available from the EBAS database infrastructure
874 (<http://ebas.nilu.no>) hosted at NILU. The research leading to these results has benefited from the
875 Aerosols, Clouds, and Trace gases Research InfraStructure (ACTRIS) network, funding from the
876 European Union Seventh Framework Programme (FP7/2007–2013) under ACTRIS-2 and grant
877 agreement no. 262254 (i.e., participation in inter-laboratory comparison for thermal–optical analysis
878 and QA and QC of measurements. S.E. and N.E. received funding from AMAP and the ABC-iCAP
879 project. Staff from the Norwegian Polar Institute are greatly acknowledged for changing of filters at the
880 Zeppelin Observatory. A.G., Z.Z. and J.D.S. thank the US National Science Foundation (NSF) under
881 Atmospheric and Geospace (AGS) Grant 2001027 for funding the synthesis of 2-methyltetrols used in
882 this study.

883

Financial support.

885 This research has been supported by the Norwegian Ministry of Climate and Environment.
886

887

References

888

889 Aas, W., Eckhardt, S., Fiebig, M., Solberg, S., and Yttri, K. E.: Monitoring of long-range transported
890 air pollutants in Norway, annual report 2019, Miljødirektoratet rapport, NILU, Kjeller, Norway, M-
891 1710/2020 NILU OR 4/2020, 2020.

892 Agrios, K., Salazar, G., Zhang, Y. L., Uglietti, C., Battaglia, M., Luginbuhl, M., Ciobanu, V. G.,
893 Vonwiller, M., and Szidat, S.: Online coupling of pure O₂ thermo-optical methods-C-14 AMS for
894 source apportionment of carbonaceous aerosols, Nuclear Instruments & Methods in Physics Research
895 Section B-Beam Interactions with Materials and Atoms, 361, 288-293, 10.1016/j.nimb.2015.06.008,
896 2015.



- 897 Ahmed, A. A., AbdelRazek, M. H., AbuMostafa, E. A., Williams, H. J., Scott, A. I., Reibenspies, J. H.,
898 and Mabry, T. J.: A new derivative of glucose and 2-C-methyl-D-erythritol from *Ferula sinaica*, *Journal*
899 *of Natural Products*, 59, 1171-1173, 1996.
- 900 Akagi, S. K., Yokelson, R. J., Wiedinmyer, C., Alvarado, M. J., Reid, J. S., Karl, T., Crounse, J. D., and
901 Wennberg, P. O.: Emission factors for open and domestic biomass burning for use in atmospheric
902 models, *Atmospheric Chemistry and Physics*, 11, 4039-4072, 10.5194/acp-11-4039-2011, 2011.
- 903 Alastuey, A., Querol, X., Aas, W., Lucarelli, F., Perez, N., Moreno, T., Cavalli, F., Areskou, H., Balan,
904 V., Catrambone, M., Ceburnis, D., Cerro, J. C., Conil, S., Gevorgyan, L., Hueglin, C., Imre, K., Jaffrezo,
905 J.-L., Leeson, S. R., Mihalopoulos, N., Mitisinkova, M., O'Dowd, C. D., Pey, J., Putaud, J.-P., Riffault,
906 V., Ripoll, A., Sciare, J., Sellegri, K., Spindler, G., and Yttri, K. E.: Geochemistry of PM10 over Europe
907 during the EMEP intensive measurement periods in summer 2012 and winter 2013, *Atmospheric*
908 *Chemistry and Physics*, 16, 6107-6129, 10.5194/acp-16-6107-2016, 2016.
- 909 Anthonsen, T., Hagen, S., Kazi, M. A., Shah, S. W., and Tagar, S.: 2-C-methyl-erythritol, a new
910 branched alditol from *convolvulus-glomeratus*, *Acta Chemica Scandinavica Series B-Organic*
911 *Chemistry and Biochemistry*, 30, 91-93, 10.3891/acta.chem.scand.30b-0091, 1976.
- 912 Anthonsen, T., Hagen, S., and Sallam, M. A. E.: Synthetic and spectroscopic studies of 2-C-methyl-
913 erythritol and 2-C-methyl-threitol, *Phytochemistry*, 19, 2375-2377, 10.1016/s0031-9422(00)91030-6,
914 1980.
- 915 Ardyna, M., Hamilton, D. S., Harmel, T., Lacour, L., Bernstein, D. N., Laliberte, J., Horvat, C.,
916 Laxenaire, R., Mills, M. M., van Dijken, G., Polyakov, I., Claustre, H., Mahowald, N., and Arrigo, K.
917 R.: Wildfire aerosol deposition likely amplified a summertime Arctic phytoplankton bloom,
918 *Communications Earth & Environment*, 3, 10.1038/s43247-022-00511-9, 2022.
- 919 Barrett, T. E., Robinson, E. M., Usenko, S., and Sheesley, R. J.: Source Contributions to Wintertime
920 Elemental and Organic Carbon in the Western Arctic Based on Radiocarbon and Tracer Apportionment,
921 *Environmental Science & Technology*, 49, 11631-11639, 10.1021/acs.est.5b03081, 2015.
- 922 Barrett, T. E., and Sheesley, R. J.: Year-round optical properties and source characterization of Arctic
923 organic carbon aerosols on the North Slope Alaska, *Journal of Geophysical Research-Atmospheres*, 122,
924 9319-9331, 10.1002/2016jd026194, 2017.
- 925 Bates, K. H., Crounse, J. D., St Clair, J. M., Bennett, N. B., Nguyen, T. B., Seinfeld, J. H., Stoltz, B. M.,
926 and Wennberg, P. O.: Gas Phase Production and Loss of Isoprene Epoxydiols, *Journal of Physical*
927 *Chemistry A*, 118, 1237-1246, 10.1021/jp4107958, 2014.
- 928 Bauer, H., Kasper-Giebl, A., Loflund, M., Giebl, H., Hitzenberger, R., Zibuschka, F., and Puxbaum, H.:
929 The contribution of bacteria and fungal spores to the organic carbon content of cloud water, precipitation
930 and aerosols, *Atmospheric Research*, 64, 109-119, 10.1016/s0169-8095(02)00084-4, 2002.
- 931 Bauer, H., Claeys, M., Vermeylen, R., Schueller, E., Weinke, G., Berger, A., and Puxbaum, H.: Arabitol
932 and mannitol as tracers for the quantification of airborne fungal spores, *Atmospheric Environment*, 42,
933 588-593, 10.1016/j.atmosenv.2007.10.013, 2008.
- 934 Bond, T. C., Doherty, S. J., Fahey, D. W., Forster, P. M., Berntsen, T., DeAngelo, B. J., Flanner, M. G.,
935 Ghan, S., Karcher, B., Koch, D., Kinne, S., Kondo, Y., Quinn, P. K., Sarofim, M. C., Schultz, M. G.,
936 Schulz, M., Venkataraman, C., Zhang, H., Zhang, S., Bellouin, N., Guttikunda, S. K., Hopke, P. K.,
937 Jacobson, M. Z., Kaiser, J. W., Klimont, Z., Lohmann, U., Schwarz, J. P., Shindell, D., Storelvmo, T.,
938 Warren, S. G., and Zender, C. S.: Bounding the role of black carbon in the climate system: A scientific
939 assessment, *Journal of Geophysical Research-Atmospheres*, 118, 5380-5552, 10.1002/jgrd.50171, 2013.



- 940 Brighty, A., Jacob, V., Uzu, G., Borlaza, L., Conil, S., Hueglin, C., Grange, S. K., Favez, O., Trebuchon,
941 C., and Jaffrezo, J. L.: Cellulose in atmospheric particulate matter at rural and urban sites across France
942 and Switzerland, *Atmospheric Chemistry and Physics*, 22, 6021-6043, 10.5194/acp-22-6021-2022,
943 2022.
- 944 Cahill, T. M., Seaman, V. Y., Charles, M. J., Holzinger, R., and Goldstein, A. H.: Secondary organic
945 aerosols formed from oxidation of biogenic volatile organic compounds in the Sierra Nevada Mountains
946 of California, *Journal of Geophysical Research-Atmospheres*, 111, 10.1029/2006jd007178, 2006.
- 947 Cassiani, M., Stohl, A., and Brioude, J.: Lagrangian Stochastic Modelling of Dispersion in the
948 Convective Boundary Layer with Skewed Turbulence Conditions and a Vertical Density Gradient:
949 Formulation and Implementation in the FLEXPART Model, *Boundary-Layer Meteorology*, 154, 367-
950 390, 10.1007/s10546-014-9976-5, 2015.
- 951 Cavalli, F., Viana, M., Yttri, K. E., Genberg, J., and Putaud, J.-P.: Toward a standardised thermal-optical
952 protocol for measuring atmospheric organic and elemental carbon: the EUSAAR protocol, *Atmospheric
953 Measurement Techniques*, 3, 79-89, 2010.
- 954 Cavalli, F., Alastuey, A., Areskou, H., Ceburnis, D., Cech, J., Genberg, J., Harrison, R. M., Jaffrezo,
955 J. L., Kiss, G., Laj, P., Mihalopoulos, N., Perez, N., Quincey, P., Schwarz, J., Sellegri, K., Spindler, G.,
956 Swietlicki, E., Theodosi, C., Yttri, K. E., Aas, W., and Putaud, J. P.: A European aerosol
957 phenomenology-4: Harmonized concentrations of carbonaceous aerosol at 10 regional background sites
958 across Europe, *Atmospheric Environment*, 144, 133-145, 10.1016/j.atmosenv.2012.07.050, 2016.
- 959 Claeys, M., Graham, B., Vas, G., Wang, W., Vermeylen, R., Pashynska, V., Cafmeyer, J., Guyon, P.,
960 Andreae, M. O., Artaxo, P., and Maenhaut, W.: Formation of secondary organic aerosols through
961 photooxidation of isoprene, *Science*, 303, 1173-1176, 10.1126/science.1092805, 2004.
- 962 Claeys, M., Kourtchev, I., Pashynska, V., Vas, G., Vermeylen, R., Wang, W., Cafmeyer, J., Chi, X.,
963 Artaxo, P., Andreae, M. O., and Maenhaut, W.: Polar organic marker compounds in atmospheric
964 aerosols during the LBA-SMOCC 2002 biomass burning experiment in Rondonia, Brazil: sources and
965 source processes, time series, diel variations and size distributions, *Atmospheric Chemistry and Physics*,
966 10, 9319-9331, 10.5194/acp-10-9319-2010, 2010.
- 967 Clarke, A. D., and Noone, K. J.: Soot in the Arctic snowpack - A cause for perturbations in radiative-
968 transfer, *Atmospheric Environment*, 19, 2045-2053, 10.1016/0004-6981(85)90113-1, 1985.
- 969 Coen, M. C., Andrews, E., Alastuey, A., Arsov, T. P., Backman, J., Brem, B. T., Bukowiecki, N., Couret,
970 C., Eleftheriadis, K., Flentje, H., Fiebig, M., Gysel-Beer, M., Hand, J. L., Hoffer, A., Hooda, R.,
971 Hueglin, C., Joubert, W., Keywood, M., Kim, J. E., Kim, S. W., Labuschagne, C., Lin, N. H., Lin, Y.,
972 Myhre, C. L., Luoma, K., Lyamani, H., Marinoni, A., Mayol-Bracero, O. L., Mihalopoulos, N., Pandolfi,
973 M., Prats, N., Prenni, A. J., Putaud, J. P., Ries, L., Reisen, F., Sellegri, K., Sharma, S., Sheridan, P.,
974 Sherman, J. P., Sun, J. Y., Titos, G., Torres, E., Tuch, T., Weller, R., Wiedensohler, A., Zieger, P., and
975 Laj, P.: Multidecadal trend analysis of in situ aerosol radiative properties around the world, *Atmospheric
976 Chemistry and Physics*, 20, 8867-8908, 10.5194/acp-20-8867-2020, 2020.
- 977 Creamean, J. M., Kirpes, R. M., Pratt, K. A., Spada, N. J., Maahn, M., de Boer, G., Schnell, R. C., and
978 China, S.: Marine and terrestrial influences on ice nucleating particles during continuous springtime
979 measurements in an Arctic oilfield location, *Atmospheric Chemistry and Physics*, 18, 18023-18042,
980 10.5194/acp-18-18023-2018, 2018.
- 981 Creamean, J. M., Mignani, C., Bukowiecki, N., and Conen, F.: Using freezing spectra characteristics to
982 identify ice-nucleating particle populations during the winter in the Alps, *Atmospheric Chemistry and
983 Physics*, 19, 8123-8140, 10.5194/acp-19-8123-2019, 2019.



- 984 Creamean, J. M., Hill, T. C. J., DeMott, P. J., Uetake, J., Kreidenweis, S., and Douglas, T. A.: Thawing
985 permafrost: an overlooked source of seeds for Arctic cloud formation, *Environmental Research Letters*,
986 15, 10.1088/1748-9326/ab87d3, 2020.
- 987 Cui, T. Q., Zeng, Z. X., dos Santos, E. O., Zhang, Z. F., Chen, Y. Z., Zhang, Y., Rose, C. A.,
988 Budisulistiorini, S. H., Collins, L. B., Bodnar, W. M., de Souza, R. A. F., Martin, S. T., Machado, C. M.
989 D., Turpin, B. J., Gold, A., Ault, A. P., and Surratt, J. D.: Development of a hydrophilic interaction
990 liquid chromatography (HILIC) method for the chemical characterization of water-soluble isoprene
991 epoxydiol (IEPOX)-derived secondary organic aerosol, *Environmental Science-Processes & Impacts*,
992 20, 1524-1536, 10.1039/c8em00308d, 2018.
- 993 Dani, K. G. S., and Loreto, F.: Trade-Off Between Dimethyl Sulfide and Isoprene Emissions from
994 Marine Phytoplankton, *Trends in Plant Science*, 22, 361-372, 10.1016/j.tplants.2017.01.006, 2017.
- 995 Darer, A. I., Cole-Filipiak, N. C., O'Connor, A. E., Elrod, M. J.: Formation and Stability of
996 Atmospherically Relevant Isoprene-Derived Organosulfates and Organonitrates, *Environ. Sci. Technol.*
997 45 (5), 1895 – 1902, <https://doi.org/10.1021/es103797z>, 2011.
- 998 Dittrich, P., and Angyal, S. J.: 2-C-methyl-erythritol in leaves of *Liriodendron-tulipifera*,
999 *Phytochemistry*, 27, 935-935, 10.1016/0031-9422(88)84125-6, 1988.
- 1000 Duvold, T., Bravo, J. M., PaleGrosdemange, C., and Rohmer, M.: Biosynthesis of 2-C-methyl-D-
1001 erythritol, a putative C-5 intermediate in the mevalonate independent pathway for isoprenoid
1002 biosynthesis, *Tetrahedron Letters*, 38, 4769-4772, 10.1016/s0040-4039(97)01045-9, 1997.
- 1003 Dye, C., and Yttri, K.: Determination of monosaccharide anhydrides in atmospheric aerosols by use of
1004 high-performance liquid chromatography combined with high-resolution mass spectrometry, *Analytical*
1005 *Chemistry*, 77, 1853-1858, 10.1021/ac049461j, 2005.
- 1006 Eckhardt, S., Hermansen, O., Grythe, H., Fiebig, M., Stebel, K., Cassiani, M., Baecklund, A., and Stohl,
1007 A.: The influence of cruise ship emissions on air pollution in Svalbard - a harbinger of a more polluted
1008 Arctic?, *Atmospheric Chemistry and Physics*, 13, 8401-8409, 10.5194/acp-13-8401-2013, 2013.
- 1009 El Haddad, I., Marchand, N., Temime-Roussel, B., Wortham, H., Piot, C., Besombes, J. L., Baduel, C.,
1010 Voisin, D., Armengaud, A., and Jaffrezo, J. L.: Insights into the secondary fraction of the organic aerosol
1011 in a Mediterranean urban area: Marseille, *Atmospheric Chemistry and Physics*, 11, 2059-2079,
1012 10.5194/acp-11-2059-2011, 2011.
- 1013 Eleftheriadis, K., Vratolis, S., and Nyeki, S.: Aerosol black carbon in the European Arctic:
1014 Measurements at Zeppelin station, Ny-Alesund, Svalbard from 1998-2007, *Geophysical Research*
1015 *Letters*, 36, 10.1029/2008gl035741, 2009.
- 1016 Enomoto, H., Kohata, K., Nakayama, M., Yamaguchi, Y., and Ichimura, K.: 2-C-methyl-D-erythritol is
1017 a major carbohydrate in petals of *Phlox subulata* possibly involved in flower development, *Journal of*
1018 *Plant Physiology*, 161, 977-980, 10.1016/j.jplph.2004.01.009, 2004.
- 1019 Feltracco, M., Barbaro, E., Tedeschi, S., Spolaor, A., Turetta, C., Vecchiato, M., Morabito, E.,
1020 Zangrando, R., Barbante, C., and Gambaro, A.: Interannual variability of sugars in Arctic aerosol:
1021 Biomass burning and biogenic inputs, *Science of the Total Environment*, 706,
1022 10.1016/j.scitotenv.2019.136089, 2020.
- 1023 Feltracco, M., Barbaro, E., Spolaor, A., Vecchiato, M., Callegaro, A., Burgay, F., Varde, M., Maffezzoli,
1024 N., Dallo, F., Scoto, F., Zangrando, R., Barbante, C., and Gambaro, A.: Year-round measurements of



- 1025 size-segregated low molecular weight organic acids in Arctic aerosol, *Science of the Total Environment*,
1026 763, 10.1016/j.scitotenv.2020.142954, 2021.
- 1027 Ferrero, L., Sangiorgi, G., Perrone, M. G., Rizzi, C., Cataldi, M., Markuszewski, P., Pakszys, P.,
1028 Makuch, P., Petelski, T., Becagli, S., Traversi, R., Bolzacchini, E., and Zielinski, T.: Chemical
1029 Composition of Aerosol over the Arctic Ocean from Summer ARctic EXpedition (AREX) 2011-2012
1030 Cruises: Ions, Amines, Elemental Carbon, Organic Matter, Polycyclic Aromatic Hydrocarbons, n-
1031 Alkanes, Metals, and Rare Earth Elements, *Atmosphere*, 10, 10.3390/atmos10020054, 2019.
- 1032 Forster, C., Stohl, A., and Seibert, P.: Parameterization of convective transport in a Lagrangian particle
1033 dispersion model and its evaluation, *Journal of Applied Meteorology and Climatology*, 46, 403-422,
1034 10.1175/jam2470.1, 2007.
- 1035 Fu, P. Q., Kawamura, K., Chen, J., and Barrie, L. A.: Isoprene, Monoterpene, and Sesquiterpene
1036 Oxidation Products in the High Arctic Aerosols during Late Winter to Early Summer, *Environmental
1037 Science & Technology*, 43, 4022-4028, 10.1021/es803669a, 2009a.
- 1038 Fu, P. Q., Kawamura, K., and Barrie, L. A.: Photochemical and Other Sources of Organic Compounds
1039 in the Canadian High Arctic Aerosol Pollution during Winter-Spring, *Environmental Science &
1040 Technology*, 43, 286-292, 10.1021/es803046q, 2009b.
- 1041 Fu, P. Q., Kawamura, K., Kanaya, Y., and Wang, Z. F.: Contributions of biogenic volatile organic
1042 compounds to the formation of secondary organic aerosols over Mt Tai, Central East China,
1043 *Atmospheric Environment*, 44, 4817-4826, 10.1016/j.atmosenv.2010.08.040, 2010.
- 1044 Fu, P. Q., Kawamura, K., Chen, J., Charriere, B., and Sempere, R.: Organic molecular composition of
1045 marine aerosols over the Arctic Ocean in summer: contributions of primary emission and secondary
1046 aerosol formation, *Biogeosciences*, 10, 653-667, 10.5194/bg-10-653-2013, 2013.
- 1047 Gelencser, A., May, B., Simpson, D., Sanchez-Ochoa, A., Kasper-Giebl, A., Puxbaum, H., Caseiro, A.,
1048 Pio, C., and Legrand, M.: Source apportionment of PM_{2.5} organic aerosol over Europe:
1049 Primary/secondary, natural/anthropogenic, and fossil/biogenic origin, *Journal of Geophysical Research-
1050 Atmospheres*, 112, 10.1029/2006jd008094, 2007.
- 1051 Genberg, J., Hyder, M., Stenstrom, K., Bergstrom, R., Simpson, D., Fors, E. O., Jonsson, J. A., and
1052 Swietlicki, E.: Source apportionment of carbonaceous aerosol in southern Sweden, *Atmospheric
1053 Chemistry and Physics*, 11, 11387-11400, 10.5194/acp-11-11387-2011, 2011.
- 1054 Giglio, L., Descloitres, J., Justice, C. O., and Kaufman, Y. J.: An enhanced contextual fire detection
1055 algorithm for MODIS, *Remote Sensing of Environment*, 87, 273-282, 10.1016/s0034-4257(03)00184-
1056 6, 2003.
- 1057 Gilardoni, S., Vignati, E., Cavalli, F., Putaud, J. P., Larsen, B. R., Karl, M., Stenstrom, K., Genberg, J.,
1058 Henne, S., and Dentener, F.: Better constraints on sources of carbonaceous aerosols using a combined
1059 C-14 - macro tracer analysis in a European rural background site, *Atmospheric Chemistry and Physics*,
1060 11, 5685-5700, 10.5194/acp-11-5685-2011, 2011.
- 1061 Gonzalez, N. J. D., Borg-Karlson, A. K., Artaxo, P., Guenther, A., Krejci, R., Noziere, B., and Noone,
1062 K.: Primary and secondary organics in the tropical Amazonian rainforest aerosols: chiral analysis of 2-
1063 methyltetraols, *Environmental Science-Processes & Impacts*, 16, 1413-1421, 10.1039/c4em00102h,
1064 2014.



- 1065 Grythe, H., Kristiansen, N. I., Zwaafink, C. D. G., Eckhardt, S., Strom, J., Tunved, P., Krejci, R., and
1066 Stohl, A.: A new aerosol wet removal scheme for the Lagrangian particle model FLEXPART v10,
1067 *Geoscientific Model Development*, 10, 1447-1466, 10.5194/gmd-10-1447-2017, 2017.
- 1068 Hallquist, M., Wenger, J. C., Baltensperger, U., Rudich, Y., Simpson, D., Claeys, M., Dommen, J.,
1069 Donahue, N. M., George, C., Goldstein, A. H., Hamilton, J. F., Herrmann, H., Hoffmann, T., Iinuma,
1070 Y., Jang, M., Jenkin, M. E., Jimenez, J. L., Kiendler-Scharr, A., Maenhaut, W., McFiggans, G., Mentel,
1071 T. F., Monod, A., Prevot, A. S. H., Seinfeld, J. H., Surratt, J. D., Szmigielski, R., and Wildt, J.: The
1072 formation, properties and impact of secondary organic aerosol: current and emerging issues,
1073 *Atmospheric Chemistry and Physics*, 9, 5155-5236, 10.5194/acp-9-5155-2009, 2009.
- 1074 Hansen, A. M. K., Kristensen, K., Nguyen, Q. T., Zare, A., Cozzi, F., Nojgaard, J. K., Skov, H., Brandt,
1075 J., Christensen, J. H., Strom, J., Tunved, P., Krejci, R., and Glasius, M.: Organosulfates and organic
1076 acids in Arctic aerosols: speciation, annual variation and concentration levels, *Atmospheric Chemistry
1077 and Physics*, 14, 7807-7823, 10.5194/acp-14-7807-2014, 2014.
- 1078 Hansen, J., and Nazarenko, L.: Soot climate forcing via snow and ice albedos, *Proceedings of the
1079 National Academy of Sciences of the United States of America*, 101, 423-428,
1080 10.1073/pnas.2237157100, 2004.
- 1081 Hartmann, M., Blunier, T., Brugger, S. O., Schmale, J., Schwikowski, M., Vogel, A., Wex, H., and
1082 Stratmann, F.: Variation of Ice Nucleating Particles in the European Arctic Over the Last Centuries,
1083 *Geophysical Research Letters*, 46, 4007-4016, 10.1029/2019gl082311, 2019.
- 1084 Hartmann, M., Adachi, K., Eppers, O., Haas, C., Herber, A., Holzinger, R., Hunerbein, A., Jakel, E.,
1085 Jentsch, C., van Pinxteren, M., Wex, H., Willmes, S., and Stratmann, F.: Wintertime Airborne
1086 Measurements of Ice Nucleating Particles in the High Arctic: A Hint to a Marine, Biogenic Source for
1087 Ice Nucleating Particles, *Geophysical Research Letters*, 47, 10.1029/2020gl087770, 2020.
- 1088 Hersbach, H., Bell, B., Berrisford, P., Hirahara, S., Horanyi, A., Muñoz-Sabater, J., Nicolas, J., Peubey,
1089 C., Radu, R., Schepers, D., Simmons, A., Soci, C., Abdalla, S., Abellan, X., Balsamo, G., Bechtold, P.,
1090 Biavati, G., Bidlot, J., Bonavita, M., De Chiara, G., Dahlgren, P., Dee, D., Diamantakis, M., Dragani,
1091 R., Flemming, J., Forbes, R., Fuentes, M., Geer, A., Haimberger, L., Healy, S., Hogan, R. J., Holm, E.,
1092 Janiskova, M., Keeley, S., Laloyaux, P., Lopez, P., Lupu, C., Radnoti, G., de Rosnay, P., Rozum, I.,
1093 Vamborg, F., Villaume, S., and Thepaut, J. N.: The ERA5 global reanalysis, *Quarterly Journal of the
1094 Royal Meteorological Society*, 146, 1999-2049, 10.1002/qj.3803, 2020.
- 1095 Heslin-Rees, D., Burgos, M., Hansson, H. C., Krejci, R., Strom, J., Tunved, P., and Zieger, P.: From a
1096 polar to a marine environment: has the changing Arctic led to a shift in aerosol light scattering
1097 properties?, *Atmospheric Chemistry and Physics*, 20, 13671-13686, 10.5194/acp-20-13671-2020, 2020.
- 1098 Hirdman, D., Sodemann, H., Eckhardt, S., Burkhart, J. F., Jefferson, A., Mefford, T., Quinn, P. K.,
1099 Sharma, S., Strom, J., and Stohl, A.: Source identification of short-lived air pollutants in the Arctic using
1100 statistical analysis of measurement data and particle dispersion model output, *Atmospheric Chemistry
1101 and Physics*, 10, 669-693, 10.5194/acp-10-669-2010, 2010.
- 1102 Hodshire, A. L., Campuzano-Jost, P., Kodros, J. K., Croft, B., Nault, B. A., Schroder, J. C., Jimenez, J.
1103 L., and Pierce, J. R.: The potential role of methanesulfonic acid (MSA) in aerosol formation and growth
1104 and the associated radiative forcings, *Atmospheric Chemistry and Physics*, 19, 3137-3160, 10.5194/acp-
1105 19-3137-2019, 2019.
- 1106 Horn, S. J., Aasen, I. M., and Ostgaard, K.: Ethanol production from seaweed extract, *Journal of
1107 Industrial Microbiology & Biotechnology*, 25, 249-254, 10.1038/sj.jim.7000065, 2000.



- 1108 Hu, Q. H., Xie, Z. Q., Wang, X. M., Kang, H., and Zhang, P. F.: Levoglucosan indicates high levels of
1109 biomass burning aerosols over oceans from the Arctic to Antarctic, *Scientific Reports*, 3, 7,
1110 10.1038/srep03119, 2013.
- 1111 Ion, A. C., Vermeylen, R., Kourtchev, I., Cafmeyer, J., Chi, X., Gelencser, A., Maenhaut, W., and
1112 Claeys, M.: Polar organic compounds in rural PM(2.5) aerosols from K-puszta, Hungary, during a 2003
1113 summer field campaign: Sources and diel variations, *Atmospheric Chemistry and Physics*, 5, 1805-1814,
1114 10.5194/acp-5-1805-2005, 2005.
- 1115 Jacobsen, E. E., and Anthonsen, T.: 2-C-Methyl-D-erythritol. Produced in plants, forms aerosols in the
1116 atmosphere. An alternative pathway in isoprenoid biosynthesis, *Biocatalysis and Biotransformation*, 33,
1117 191-196, 10.3109/10242422.2015.1095677, 2015.
- 1118 Jiao, C. Y., and Flanner, M. G.: Changing black carbon transport to the Arctic from present day to the
1119 end of 21st century, *Journal of Geophysical Research-Atmospheres*, 121, 4734-4750,
1120 10.1002/2015jd023964, 2016.
- 1121 Jurányi, Z., Zanatta, M., Lund, M.T., Samset, B.H., Skeie, R.B., Sharma, S., Wendisch, M., Herber, A.:
1122 Atmospheric concentrations of black carbon are substantially higher in spring than summer in the Arctic.
1123 *Communications Earth & Environment* 4, 91, 2023. <https://doi.org/10.1038/s43247-023-00749-x>.
- 1124 Karl, M., Leck, C., Coz, E., and Heintzenberg, J.: Marine nanogels as a source of atmospheric
1125 nanoparticles in the high Arctic, *Geophysical Research Letters*, 40, 3738-3743, 10.1002/grl.50661,
1126 2013.
- 1127 Karlsen, S. R., Elvebakk, A., Hogda, K. A., and Grydeland, T.: Spatial and Temporal Variability in the
1128 Onset of the Growing Season on Svalbard, Arctic Norway - Measured by MODIS-NDVI Satellite Data,
1129 *Remote Sensing*, 6, 8088-8106, 10.3390/rs6098088, 2014.
- 1130 Klimont, Z., Kupiainen, K., Heyes, C., Purohit, P., Cofala, J., Rafaj, P., Borcen-Kleefeld, J., and Schopp,
1131 W.: Global anthropogenic emissions of particulate matter including black carbon, *Atmospheric
1132 Chemistry and Physics*, 17, 8681-8723, 10.5194/acp-17-8681-2017, 2017.
- 1133 Kourtchev, I., Ruuskanen, T., Maenhaut, W., Kulmala, M., and Claeys, M.: Observation of 2-
1134 methyltetrols and related photo-oxidation products of isoprene in boreal forest aerosols from Hyytiälä,
1135 Finland, *Atmospheric Chemistry and Physics*, 5, 2761-2770, 10.5194/acp-5-2761-2005, 2005.
- 1136 Kourtchev, I., Ruuskanen, T. M., Keronen, P., Sogacheva, L., Dal Maso, M., Reissell, A., Chi, X.,
1137 Vermeylen, R., Kulmala, M., Maenhaut, W., and Claeys, M.: Determination of isoprene and alpha-/beta-
1138 pinene oxidation products in boreal forest aerosols from Hyytiälä, Finland: diel variations and possible
1139 link with particle formation events, *Plant Biology*, 10, 138-149, 10.1055/s-2007-964945, 2008a.
- 1140 Kourtchev, I., Warnke, J., Maenhaut, W., Hoffmann, T., and Claeys, M.: Polar organic marker
1141 compounds in PM2.5 aerosol from a mixed forest site in western Germany, *Chemosphere*, 73, 1308-
1142 1314, 10.1016/j.chemosphere.2008.07.011, 2008b.
- 1143 Kramshoj, M., Vedel-Petersen, I., Schollert, M., Rinnan, A., Nymand, J., Ro-Poulsen, H., and Rinnan,
1144 R.: Large increases in Arctic biogenic volatile emissions are a direct effect of warming, *Nature
1145 Geoscience*, 9, 349+, 10.1038/ngeo2692, 2016.
- 1146 Kunit, M., and Puxbaum, H.: Enzymatic determination of the cellulose content of atmospheric aerosols,
1147 *Atmospheric Environment*, 30, 1233-1236, 10.1016/1352-2310(95)00429-7, 1996.



- 1148 Li, S. M., Barrie, L. A., and Sirois, A.: Biogenic sulfur aerosol in the Arctic troposphere. 2. Trends and
1149 seasonal-variations, *Journal of Geophysical Research-Atmospheres*, 98, 20623-20631,
1150 10.1029/93jd02233, 1993.
- 1151 Liakakou, E., Vrekoussis, M., Bonsang, B., Donousis, C., Kanakidou, M., and Mihalopoulos, N.:
1152 Isoprene above the Eastern Mediterranean: Seasonal variation and contribution to the oxidation capacity
1153 of the atmosphere, *Atmospheric Environment*, 41, 1002-1010, 10.1016/j.atmosenv.2006.09.034, 2007.
- 1154 Lin, Y. H., Zhang, Z. F., Docherty, K. S., Zhang, H. F., Budisulistiorini, S. H., Rubitschun, C. L.,
1155 Shaw, S. L., Knipping, E. M., Edgerton, E. S., Kleindienst, T. E., Gold, A., and Surratt, J. D.: Isoprene
1156 Epoxydiols as Precursors to Secondary Organic Aerosol Formation: Acid-Catalyzed Reactive Uptake
1157 Studies with Authentic Compounds, *Environmental Science & Technology*, 46, 250-258,
1158 10.1021/es202554c, 2012.
- 1159 Long, C. M., Nascarella, M. A., and Valberg, P. A.: Carbon black vs. black carbon and other airborne
1160 materials containing elemental carbon: Physical and chemical distinctions, *Environmental Pollution*,
1161 181, 271-286, 10.1016/j.envpol.2013.06.009, 2013.
- 1162 Lopez-Hilfiker, F. D., Mohr, C., D'Ambro, E. L., Lutz, A., Riedel, T. P., Gaston, C. J., Iyer, S., Zhang,
1163 Z., Gold, A., Surratt, J. D., Lee, B. H., Kurten, T., Hu, W. W., Jimenez, J., Hallquist, M., and Thornton,
1164 J. A.: Molecular Composition and Volatility of Organic Aerosol in the Southeastern US: Implications
1165 for IEPDX Derived SOA, *Environmental Science & Technology*, 50, 2200-2209,
1166 10.1021/acs.est.5b04769, 2016.
- 1167 McCarty, J. L., Aalto, J., Paunu, V. V., Arnold, S. R., Eckhardt, S., Klimont, Z., Fain, J. J., Evangelidou,
1168 N., Venalainen, A., Tchepakova, N. M., Parfenova, E. I., Kupiainen, K., Soja, A. J., Huang, L., and
1169 Wilson, S.: Reviews and syntheses: Arctic fire regimes and emissions in the 21st century,
1170 *Biogeosciences*, 18, 5053-5083, 10.5194/bg-18-5053-2021, 2021.
- 1171 McDow, S. R., and Huntzicker, J. J.: Organic Aerosol Sampling Artifacts, *Abstracts of Papers of the*
1172 *American Chemical Society*, 200, 106-Envr, 1990.
- 1173 McFiggans, G., Mentel, T. F., Wildt, J., Pullinen, I., Kang, S., Kleist, E., Schmitt, S., Springer, M.,
1174 Tillmann, R., Wu, C., Zhao, D. F., Hallquist, M., Faxon, C., Le Breton, M., Hallquist, A. M., Simpson,
1175 D., Bergstrom, R., Jenkin, M. E., Ehn, M., Thornton, J. A., Alfarra, M. R., Bannan, T. J., Percival, C.
1176 J., Priestley, M., Topping, D., and Kiendler-Scharr, A.: Secondary organic aerosol reduced by mixture
1177 of atmospheric vapours, *Nature*, 565, 587-593, 10.1038/s41586-018-0871-y, 2019.
- 1178
- 1179 Medeiros, P. M., Conte, M. H., Weber, J. C., and Simoneit, B. R. T.: Sugars as source indicators of
1180 biogenic organic carbon in aerosols collected above the Howland Experimental Forest, Maine,
1181 *Atmospheric Environment*, 40, 1694-1705, 10.1016/j.atmosenv.2005.11.001, 2006.
- 1182 Moschos, V., Dzepina, K., Bhattu, D., Lamkaddam, H., Casotto, R., Daellenbach, K. R., Canonaco, F.,
1183 Rai, P., Aas, W., Becagli, S., Calzolari, G., Eleftheriadis, K., Moffett, C. E., Schnelle-Kreis, J., Severi,
1184 M., Sharma, S., Skov, H., Vestenius, M., Zhang, W., Hakola, H., Hellén, H., Huang, L., Jaffrezou, J.-L.,
1185 Massling, A., Nøjgaard, J. K., Petäjä, T., Popovicheva, O., Sheesley, R. J., Traversi, R., Yttri, K. E.,
1186 Schmale, J., Prévôt, A. S. H., Baltensperger, U., and El Haddad, I.: Equal abundance of summertime
1187 natural and wintertime anthropogenic Arctic organic aerosols, *Nature Geoscience*, 10.1038/s41561-021-
1188 00891-1, 2022.
- 1189 Myers-Smith, I. H., Kerby, J. T., Phoenix, G. K., Bjerke, J. W., Epstein, H. E., Assmann, J. J., John, C.,
1190 Andreu-Hayles, L., Angers-Blondin, S., Beck, P. S. A., Berner, L. T., Bhatt, U. S., Bjorkman, A. D.,



- 1191 Blok, D., Bryn, A., Christiansen, C. T., Cornelissen, J. H. C., Cunliffe, A. M., Elmendorf, S. C., Forbes,
1192 B. C., Goetz, S. J., Hollister, R. D., de Jong, R., Lorant, M. M., Macias-Fauria, M., Maseyk, K.,
1193 Normand, S., Olofsson, J., Parker, T. C., Parmentier, F. J. W., Post, E., Schaepman-Strub, G., Stordal,
1194 F., Sullivan, P. F., Thomas, H. J. D., Tømmervik, H., Treharne, R., Tweedie, C. E., Walker, D. A.,
1195 Wilmking, M., and Wipf, S.: Complexity revealed in the greening of the Arctic, *Nature Climate Change*,
1196 10, 106-117, 10.1038/s41558-019-0688-1, 2020.
- 1197 Ng, N. L., Brown, S. S., Archibald, A. T., Atlas, E., Cohen, R. C., Crowley, J. N., Day, D. A., Donahue,
1198 N. M., Fry, J. L., Fuchs, H., Griffin, R. J., Guzman, M. I., Herrmann, H., Hodzic, A., Iinuma, Y.,
1199 Jimenez, J. L., Kiendler-Scharr, A., Lee, B. H., Luecken, D. J., Mao, J. Q., McLaren, R., Mutzel, A.,
1200 Osthoff, H. D., Ouyang, B., Picquet-Varrault, B., Platt, U., Pye, H. O. T., Rudich, Y., Schwantes, R. H.,
1201 Shiraiwa, M., Stutz, J., Thornton, J. A., Tilgner, A., Williams, B. J., and Zaveri, R. A.: Nitrate radicals
1202 and biogenic volatile organic compounds: oxidation, mechanisms, and organic aerosol, *Atmospheric
1203 Chemistry and Physics*, 17, 2103-2162, 10.5194/acp-17-2103-2017, 2017.
- 1204 Nolte, C. G., Schauer, J. J., Cass, G. R., and Simoneit, B. R. T.: Highly polar organic compounds present
1205 in wood smoke and in the ambient atmosphere, *Environmental Science & Technology*, 35, 1912-1919,
1206 10.1021/es001420r, 2001.
- 1207 Noziere, B., Gonzalez, N. J. D., Borg-Karlson, A. K., Pei, Y. X., Redeby, J. P., Krejci, R., Dommen, J.,
1208 Prevot, A. S. H., and Anthonsen, T.: Atmospheric chemistry in stereo: A new look at secondary organic
1209 aerosols from isoprene, *Geophysical Research Letters*, 38, 10.1029/2011gl047323, 2011.
- 1210 Noziere, B., Kalberer, M., Claeys, M., Allan, J., D'Anna, B., Decesari, S., Finessi, E., Glasius, M., Grgic,
1211 I., Hamilton, J. F., Hoffmann, T., Iinuma, Y., Jaoui, M., Kahno, A., Kampf, C. J., Kourtchev, I.,
1212 Maenhaut, W., Marsden, N., Saarikoski, S., Schnelle-Kreis, J., Surratt, J. D., Szidat, S., Szmigielski, R.,
1213 and Wisthaler, A.: The Molecular Identification of Organic Compounds in the Atmosphere: State of the
1214 Art and Challenges, *Chemical Reviews*, 115, 3919-3983, 10.1021/cr5003485, 2015a.
- 1215 Ottar, B.: Arctic air-pollution - A Norwegian Perspective, *Atmospheric Environment*, 23, 2349-2356,
1216 10.1016/0004-6981(89)90248-5, 1989.
- 1217 Paasonen, P., Asmi, A., Petaja, T., Kajos, M. K., Aijala, M., Junninen, H., Holst, T., Abbatt, J. P. D.,
1218 Arneth, A., Birmili, W., van der Gon, H. D., Hamed, A., Hoffer, A., Laakso, L., Laaksonen, A., Leaitch,
1219 Paulot, F., Crounse, J. D., Kjaergaard, H. G., Kurten, A., St Clair, J. M., Seinfeld, J. H., and Wennberg,
1220 P. O.: Unexpected Epoxide Formation in the Gas-Phase Photooxidation of Isoprene, *Science*, 325, 730-
1221 733, 10.1126/science.1172910, 2009.
- 1222 W. R., Plass-Dulmer, C., Pryor, S. C., Raisanen, P., Swietlicki, E., Wiedensohler, A., Worsnop, D. R.,
1223 Kerminen, V. M., and Kulmala, M.: Warming-induced increase in aerosol number concentration likely
1224 to moderate climate change, *Nature Geoscience*, 6, 438-442, 10.1038/ngeo1800, 2013.
- 1225 Pisso, I., Sollum, E., Grythe, H., Kristiansen, N. I., Cassiani, M., Eckhardt, S., Arnold, D., Morton, D.,
1226 Thompson, R. L., Zwaftink, C. D. G., Evangeliou, N., Sodemann, H., Haimberger, L., Henne, S.,
1227 Brunner, D., Burkhardt, J. F., Fouilloux, A., Brioude, J., Philipp, A., Seibert, P., and Stohl, A.: The
1228 Lagrangian particle dispersion model FLEXPART version 10.4, *Geoscientific Model Development*, 12,
1229 4955-4997, 10.5194/gmd-12-4955-2019, 2019.
- 1230 Platt, S. M., Hov, O., Berg, T., Breivik, K., Eckhardt, S., Eleftheriadis, K., Evangeliou, N., Fiebig, M.,
1231 Fisher, R., Hansen, G., Hansson, H. C., Heintzenberg, J., Hermansen, O., Heslin-Rees, D., Holmen, K.,
1232 Hudson, S., Kallenborn, R., Krejci, R., Krognes, T., Larssen, S., Lowry, D., Myhre, C. L., Lunder, C.,
1233 Nisbet, E., Nizzetto, P. B., Park, K. T., Pedersen, C. A., Pfaffhuber, K. A., Rockmann, T., Schmidbauer,
1234 N., Solberg, S., Stohl, A., Strom, J., Svendby, T., Tunved, P., Tornkvist, K., van der Veen, C., Vratolis,



- 1235 S., Yoon, Y. J., Yttri, K. E., Zieger, P., Aas, W., and Torseth, K.: Atmospheric composition in the
1236 European Arctic and 30 years of the Zeppelin Observatory, Ny-Ålesund, *Atmospheric Chemistry and*
1237 *Physics*, 22, 3321-3369, 10.5194/acp-22-3321-2022, 2022.
- 1238 Platt, S. M., et al.: Source apportionment of equivalent black carbon from the winter 2017–2018 EMEP
1239 intensive measurement campaign using PMF, in preparation, 2023.
- 1240 Prospero, J. M., Blades, E., Mathison, G., and Naidu, R.: Interhemispheric transport of viable fungi and
1241 bacteria from Africa to the Caribbean with soil dust, *Aerobiologia*, 21, 1-19, 10.1007/s10453-004-5872-
1242 7, 2005.
- 1243 Pueschel, R. F., and Kinne, S. A.: Physical and radiative properties of Arctic atmospheric aerosols,
1244 *Science of the Total Environment*, 160-61, 811-824, 10.1016/0048-9697(95)04414-v, 1995.
- 1245 Puxbaum, H., and Tenze-Kunit, M.: Size distribution and seasonal variation of atmospheric cellulose,
1246 *Atmospheric Environment*, 37, 3693-3699, 10.1016/s1352-2310(03)00451-5, 2003.
- 1247 Qi, L., Vogel, A. L., Esmaeilirad, S., Cao, L. M., Zheng, J., Jaffrezo, J. L., Fermo, P., Kasper-Giebl, A.,
1248 Daellenbach, K. R., Chen, M. D., Ge, X. L., Baltensperger, U., Prevot, A. S. H., and Slowik, J. G.: A 1-
1249 year characterization of organic aerosol composition and sources using an extractive electrospray
1250 ionization time-of-flight mass spectrometer (EESI-TOF), *Atmospheric Chemistry and Physics*, 20,
1251 7875-7893, 10.5194/acp-20-7875-2020, 2020.
- 1252 Quinn, P. K., Miller, T. L., Bates, T. S., Ogren, J. A., Andrews, E., and Shaw, G. E.: A 3-year record of
1253 simultaneously measured aerosol chemical and optical properties at Barrow, Alaska, *Journal of*
1254 *Geophysical Research-Atmospheres*, 107, 10.1029/2001jd001248, 2002.
- 1255 Quinn, P. K., Shaw, G., Andrews, E., Dutton, E. G., Ruoho-Airola, T., and Gong, S. L.: Arctic haze:
1256 current trends and knowledge gaps, *Tellus Series B-Chemical and Physical Meteorology*, 59, 99-114,
1257 10.1111/j.1600-0889.2006.00238.x, 2007.
- 1258 Quinn, P. K., Bates, T. S., Schulz, K., and Shaw, G. E.: Decadal trends in aerosol chemical composition
1259 at Barrow, Alaska: 1976-2008, *Atmospheric Chemistry and Physics*, 9, 8883-8888, 10.5194/acp-9-
1260 8883-2009, 2009.
- 1261 Rauber, M., Salazar, G., Yttri, K. E., and Szidat, S.: An optimised organic carbon/elemental carbon
1262 (OC/EC) fraction separation method for radiocarbon source apportionment applied to low-loaded
1263 Arctic aerosol filters, *Atmos. Meas. Tech.*, 16, 825–844, <https://doi.org/10.5194/amt-16-825-2023>,
1264 2023.
1265
- 1266 Rauber, M. et al.: Organic aerosols at Trollhaugen Observatory (Antarctica) in summer are dominated
1267 by marine sources. In preparation, 2023.
- 1268 Ricard, V., Jaffrezo, J. L., Kerminen, V. M., Hillamo, R. E., Sillanpaa, M., Ruellan, S., Liousse, C., and
1269 Cachier, H.: Two years of continuous aerosol measurements in northern Finland, *Journal of Geophysical*
1270 *Research-Atmospheres*, 107, 10.1029/2001jd000952, 2002.
- 1271 Riipinen, I., Pierce, J. R., Yli-Juuti, T., Nieminen, T., Hakkinen, S., Ehn, M., Junninen, H., Lehtipalo,
1272 K., Petaja, T., Slowik, J., Chang, R., Shantz, N. C., Abbatt, J., Leaitch, W. R., Kerminen, V. M.,
1273 Worsnop, D. R., Pandis, S. N., Donahue, N. M., and Kulmala, M.: Organic condensation: a vital link
1274 connecting aerosol formation to cloud condensation nuclei (CCN) concentrations, *Atmospheric*
1275 *Chemistry and Physics*, 11, 3865-3878, 10.5194/acp-11-3865-2011, 2011.



- 1276 Rotzer, T., and Chmielewski, F. M.: Phenological maps of Europe, *Climate Research*, 18, 249-257,
1277 10.3354/cr018249, 2001.
- 1278 Sagner, S., Eisenreich, W., Fellermeier, M., Latzel, C., Bacher, A., and Zenk, M. H.: Biosynthesis of 2-
1279 C-methyl-D-erythritol in plants by rearrangement of the terpenoid precursor, 1-deoxy-D-xylulose 5-
1280 phosphate, *Tetrahedron Letters*, 39, 2091-2094, 10.1016/s0040-4039(98)00296-2, 1998.
- 1281 Samake, A., Jaffrezo, J. L., Favez, O., Weber, S., Jacob, V., Canete, T., Albinet, A., Charron, A.,
1282 Riffault, V., Perdrix, E., Waked, A., Golly, B., Salameh, D., Chevrier, F., Oliveira, D. M., Besombes, J.
1283 L., Martins, J. M. F., Bonnaire, N., Conil, S., Guillaud, G., Mesbah, B., Rocq, B., Robic, P. Y., Hulin,
1284 A., Le Meur, S., Descheemaeker, M., Chretien, E., Marchand, N., and Uzu, G.: Arabitol, mannitol, and
1285 glucose as tracers of primary biogenic organic aerosol: the influence of environmental factors on
1286 ambient air concentrations and spatial distribution over France, *Atmospheric Chemistry and Physics*,
1287 19, 11013-11030, 10.5194/acp-19-11013-2019, 2019.
- 1288 Samake, A., Bonin, A., Jaffrezo, J. L., Taberlet, P., Weber, S., Uzu, G., Jacob, V., Conil, S., and Martins,
1289 J. M. F.: High levels of primary biogenic organic aerosols are driven by only a few plant-associated
1290 microbial taxa, *Atmospheric Chemistry and Physics*, 20, 5609-5628, 10.5194/acp-20-5609-2020, 2020.
- 1291 Sanchez-Ochoa, A., Kasper-Giebl, A., Puxbaum, H., Gelencser, A., Legrand, M., and Pio, C.:
1292 Concentration of atmospheric cellulose: A proxy for plant debris across a west-east transect over Europe,
1293 *Journal of Geophysical Research-Atmospheres*, 112, 10.1029/2006jd008180, 2007.
- 1294 Schmale, J., Zieger, P., and Ekman, A. M. L.: Aerosols in current and future Arctic climate, *Nature*
1295 *Climate Change*, 11, 95-105, 10.1038/s41558-020-00969-5, 2021.
- 1296 Schmidl, C., Marr, L. L., Caseiro, A., Kotianova, P., Berner, A., Bauer, H., Kasper-Giebl, A., and
1297 Puxbaum, H.: Chemical characterisation of fine particle emissions from wood stove combustion of
1298 common woods growing in mid-European Alpine regions, *Atmospheric Environment*, 42, 126-141,
1299 10.1016/j.atmosenv.2007.09.028, 2008.
- 1300 Serreze, M. C., and Barry, R. G.: Processes and impacts of Arctic amplification: A research synthesis,
1301 *Global and Planetary Change*, 77, 85-96, 10.1016/j.gloplacha.2011.03.004, 2011.
- 1302 Sharma, S., Chan, E., Ishizawa, M., Toom-Saunty, D., Gong, S. L., Li, S. M., Tarasick, D. W., Leaitch,
1303 W. R., Norman, A., Quinn, P. K., Bates, T. S., Lefebvre, M., Barrie, L. A., and Maenhaut, W.: Influence
1304 of transport and ocean ice extent on biogenic aerosol sulfur in the Arctic atmosphere, *Journal of*
1305 *Geophysical Research-Atmospheres*, 117, 10.1029/2011jd017074, 2012.
- 1306 Sharma, S., Barrie, L. A., Magnusson, E., Brattstrom, G., Leaitch, W. R., Steffen, A., and Landsberger,
1307 S.: A Factor and Trends Analysis of Multidecadal Lower Tropospheric Observations of Arctic Aerosol
1308 Composition, Black Carbon, Ozone, and Mercury at Alert, Canada, *Journal of Geophysical Research-*
1309 *Atmospheres*, 124, 14133-14161, 10.1029/2019jd030844, 2019.
- 1310 Shaw, G. E.: The arctic haze phenomenon, *Bulletin of the American Meteorological Society*, 76, 2403-
1311 2413, 10.1175/1520-0477(1995)076<2403:tahp>2.0.co;2, 1995.
- 1312 Simpson, D., Yttri, K. E., Klimont, Z., Kupiainen, K., Caseiro, A., Gelencser, A., Pio, C., Puxbaum, H.,
1313 and Legrand, M.: Modeling carbonaceous aerosol over Europe: Analysis of the CARBOSOL and EMEP
1314 EC/OC campaigns, *Journal of Geophysical Research-Atmospheres*, 112, 10.1029/2006JD008158, 2007.
- 1315 Solomon, A., de Boer, G., Creamean, J. M., McComiskey, A., Shupe, M. D., Maahn, M., and Cox, C.:
1316 The relative impact of cloud condensation nuclei and ice nucleating particle concentrations on phase



- 1317 partitioning in Arctic mixed-phase stratocumulus clouds, *Atmospheric Chemistry and Physics*, 18,
1318 17047-17059, 10.5194/acp-18-17047-2018, 2018.
- 1319 Stohl, A., Forster, C., Frank, A., Seibert, P., and Wotawa, G.: Technical note: The Lagrangian particle
1320 dispersion model FLEXPART version 6.2, *Atmospheric Chemistry and Physics*, 5, 2461-2474,
1321 10.5194/acp-5-2461-2005, 2005.
- 1322 Stohl, A., Andrews, E., Burkhardt, J. F., Forster, C., Herber, A., Hoch, S. W., Kowal, D., Lunder, C.,
1323 Mefford, T., Ogren, J. A., Sharma, S., Spichtinger, N., Stebel, K., Stone, R., Strom, J., Torseth, K.,
1324 Wehrli, C., and Yttri, K. E.: Pan-Arctic enhancements of light absorbing aerosol concentrations due to
1325 North American boreal forest fires during summer 2004, *Journal of Geophysical Research-
1326 Atmospheres*, 111, 10.1029/2006JD007216, 2006.
- 1327 Stohl, A., Berg, T., Burkhardt, J. F., Fjaeraa, A. M., Forster, C., Herber, A., Hov, O., Lunder, C.,
1328 McMillan, W. W., Oltmans, S., Shiobara, M., Simpson, D., Solberg, S., Stebel, K., Strom, J., Torseth,
1329 K., Treffeisen, R., Virkkunen, K., and Yttri, K. E.: Arctic smoke - record high air pollution levels in the
1330 European Arctic due to agricultural fires in Eastern Europe in spring 2006, *Atmospheric Chemistry and
1331 Physics*, 7, 511-534, 2007.
- 1332 Stohl, A., Klimont, Z., Eckhardt, S., Kupiainen, K., Shevchenko, V. P., Kopeikin, V. M., and
1333 Novigatsky, A. N.: Black carbon in the Arctic: the underestimated role of gas flaring and residential
1334 combustion emissions, *Atmospheric Chemistry and Physics*, 13, 8833-8855, 10.5194/acp-13-8833-
1335 2013, 2013.
- 1336 Surratt, J. D., Chan, A. W. H., Eddingsaas, N. C., Chan, M. N., Loza, C. L., Kwan, A. J., Hersey, S. P.,
1337 Flagan, R. C., Wennberg, P. O., and Seinfeld, J. H.: Reactive intermediates revealed in secondary
1338 organic aerosol formation from isoprene, *Proceedings of the National Academy of Sciences of the
1339 United States of America*, 107, 6640-6645, 10.1073/pnas.0911114107, 2010.
- 1340 Tobo, Y., Adachi, K., DeMott, P. J., Hill, T. C. J., Hamilton, D. S., Mahowald, N. M., Nagatsuka, N.,
1341 Ohata, S., Uetake, J., Kondo, Y., and Koike, M.: Glacially sourced dust as a potentially significant
1342 source of ice nucleating particles, *Nature Geoscience*, 12, 253-+, 10.1038/s41561-019-0314-x, 2019.
- 1343 Tonon, T., Li, Y., and McQueen-Mason, S.: Mannitol biosynthesis in algae: more widespread and
1344 diverse than previously thought, *New Phytologist*, 213, 1573-1579, 10.1111/nph.14358, 2017.
- 1345 Turpin, B. J., and Lim, H. J.: Species contributions to PM_{2.5} mass concentrations: Revisiting common
1346 assumptions for estimating organic mass, *Aerosol Science and Technology*, 35, 602-610,
1347 10.1080/02786820119445, 2001.
- 1348 van der Werf, G. R., Randerson, J. T., Giglio, L., van Leeuwen, T. T., Chen, Y., Rogers, B. M., Mu, M.
1349 Q., van Marle, M. J. E., Morton, D. C., Collatz, G. J., Yokelson, R. J., and Kasibhatla, P. S.: Global fire
1350 emissions estimates during 1997-2016, *Earth System Science Data*, 9, 697-720, 10.5194/essd-9-697-
1351 2017, 2017.
- 1352 Vegetation in Svalbard: <https://www.npolar.no/en/themes/vegetation-svalbard/>, last access: 9 February
1353 2023.
- 1354 von Schneidemesser, E., Schauer, J. J., Hagler, G. S. W., and Bergin, M. H.: Concentrations and sources
1355 of carbonaceous aerosol in the atmosphere of Summit, Greenland, *Atmospheric Environment*, 43, 4155-
1356 4162, 10.1016/j.atmosenv.2009.05.043, 2009.
- 1357 Waked, A., Favez, O., Alleman, L. Y., Piot, C., Petit, J. E., Delaunay, T., Verlinden, E., Golly, B.,
1358 Besombes, J. L., Jaffrezo, J. L., and Leoz-Garziandia, E.: Source apportionment of PM₁₀ in a north-



- 1359 western Europe regional urban background site (Lens, France) using positive matrix factorization and
1360 including primary biogenic emissions, *Atmospheric Chemistry and Physics*, 14, 3325-3346,
1361 10.5194/acp-14-3325-2014, 2014.
- 1362 Wennberg, P. O., Bates, K. H., Crouse, J. D., Dodson, L. G., McVay, R. C., Mertens, L. A., Nguyen,
1363 T. B., Praske, E., Schwantes, R. H., Smarte, M. D., St Clair, J. M., Teng, A. P., Zhang, X., and Seinfeld,
1364 J. H.: Gas-Phase Reactions of Isoprene and Its Major Oxidation Products, *Chemical Reviews*, 118, 3337-
1365 3390, 10.1021/acs.chemrev.7b00439, 2018.
- 1366 Winiger, P., Andersson, A., Yttri, K. E., Tunved, P., and Gustafsson, O.: Isotope-Based Source
1367 Apportionment of EC Aerosol Particles during Winter High-Pollution Events at the Zeppelin
1368 Observatory, Svalbard, *Environmental Science & Technology*, 49, 11959-11966,
1369 10.1021/acs.est.5b02644, 2015.
- 1370 Williams, J. and Koppmann, R.J. (2007) Volatile organic compounds in the atmosphere: An overview.
1371 In: *Volatile organic compounds in the atmosphere*. Ed. by: R. Koppmann. Oxford, Blackwell Publishing.
1372 pp. 1-19.
- 1373 Winiger, P., Barrett, T. E., Sheesley, R. J., Huang, L., Sharma, S., Barrie, L. A., Yttri, K. E., Evangeliou,
1374 N., Eckhardt, S., Stohl, A., Klimont, Z., Heyes, C., Semiletov, I. P., Dudarev, O. V., Charkin, A.,
1375 Shakhova, N., Holmstrand, H., Andersson, A., and Gustafsson, O.: Source apportionment of circum-
1376 Arctic atmospheric black carbon from isotopes and modeling, *Science Advances*, 5,
1377 10.1126/sciadv.aau8052, 2019.
- 1378 Xia, X., and Hopke, P. K.: Seasonal variation of 2-methyltetrols in ambient air samples, *Environmental
1379 Science & Technology*, 40, 6934-6937, 10.1021/es0609881, 2006.
- 1380 Yttri, K. E., Aas, W., Bjerke, A., Cape, J. N., Cavalli, F., Ceburnis, D., Dye, C., Emblico, L., Facchini,
1381 M. C., Forster, C., Hanssen, J. E., Hansson, H. C., Jennings, S. G., Maenhaut, W., Putaud, J. P., and
1382 Torseth, K.: Elemental and organic carbon in PM₁₀: a one year measurement campaign within the
1383 European Monitoring and Evaluation Programme EMEP, *Atmospheric Chemistry and Physics*, 7, 5711-
1384 5725, 2007b.
- 1385 Yttri, K. E., Dye, C., and Kiss, G.: Ambient aerosol concentrations of sugars and sugar-alcohols at four
1386 different sites in Norway, *Atmospheric Chemistry and Physics*, 7, 4267-4279, 2007a.
- 1387 Yttri, K. E., Simpson, D., Nojgaard, J. K., Kristensen, K., Genberg, J., Stenstrom, K., Swietlicki, E.,
1388 Hillamo, R., Aurela, M., Bauer, H., Offenberg, J. H., Jaoui, M., Dye, C., Eckhardt, S., Burkhardt, J. F.,
1389 Stohl, A., and Glasius, M.: Source apportionment of the summer time carbonaceous aerosol at Nordic
1390 rural background sites, *Atmospheric Chemistry and Physics*, 11, 13339-13357, 10.5194/acp-11-13339-
1391 2011, 2011b.
- 1392 Yttri, K. E., Simpson, D., Stenstrom, K., Puxbaum, H., and Svendby, T.: Source apportionment of the
1393 carbonaceous aerosol in Norway - quantitative estimates based on C-14, thermal-optical and organic
1394 tracer analysis, *Atmospheric Chemistry and Physics*, 11, 9375-9394, 10.5194/acp-11-9375-2011, 2011a.
- 1395 Yttri, K. E., Myhre, C. L., Eckhardt, S., Fiebig, M., Dye, C., Hirdman, D., Stroem, J., Klimont, Z., and
1396 Stohl, A.: Quantifying black carbon from biomass burning by means of levoglucosan - a one-year time
1397 series at the Arctic observatory Zeppelin, *Atmospheric Chemistry and Physics*, 14, 6427-6442,
1398 10.5194/acp-14-6427-2014, 2014.
- 1399 Yttri, K. E., Canonaco, F., Eckhardt, S., Evangeliou, N., Fiebig, M., Gundersen, H., Hjellbrekke, A. G.,
1400 Myhre, C. L., Platt, S. M., Prevot, A. S. H., Simpson, D., Solberg, S., Surratt, J., Torseth, K., Uggerud,
1401 H., Vadset, M., Wan, X., and Aas, W.: Trends, composition, and sources of carbonaceous aerosol at the



- 1402 Birkenes Observatory, northern Europe, 2001-2018, *Atmospheric Chemistry and Physics*, 21, 7149-
1403 7170, 10.5194/acp-21-7149-2021, 2021.
- 1404 Zangrando, R., Barbaro, E., Zennaro, P., Rossi, S., Kehrwald, N. M., Gabrieli, J., Barbante, C., and
1405 Gambaro, A.: Molecular Markers of Biomass Burning in Arctic Aerosols, *Environmental Science &*
1406 *Technology*, 47, 8565-8574, 10.1021/es400125r, 2013.
- 1407 Zwaafink, C. D. G., Grythe, H., Skov, H., and Stohl, A.: Substantial contribution of northern high-
1408 latitude sources to mineral dust in the Arctic, *Journal of Geophysical Research-Atmospheres*, 121,
1409 13678-13697, 10.1002/2016jd025482, 2016.
- 1410 Zwaafink, C. D. G., Aas, W., Eckhardt, S., Evangeliou, N., Hamer, P., Johnsrud, M., Kylling, A., Platt,
1411 S. M., Stebel, K., Uggerud, H., and Yttri, K. E.: What caused a record high PM₁₀ episode in northern
1412 Europe in October 2020?, *Atmospheric Chemistry and Physics*, 22, 3789-3810, 10.5194/acp-22-3789-
1413 2022, 2022.



Table 1: Annual and seasonal mean concentrations of OC, OC_b, EC, TC, and organic tracers at Zeppelin Observatory, 2017 to 2020.

	OC (ng C m ⁻³)	OC _b (ng C m ⁻³)	EC (ng C m ⁻³)	TC (ng C m ⁻³)	Cellul. (ng m ⁻³)	Levo-gl. (pg m ⁻³)	Mannos. (pg m ⁻³)	Galactos. (pg m ⁻³)	Arabitol (pg m ⁻³)	Mannitol (pg m ⁻³)	Fructose (pg m ⁻³)	Glucose (pg m ⁻³)	Trehalose (pg m ⁻³)	2-methylery. (pg m ⁻³)	2-methylth. (pg m ⁻³)
2017	121	32.9	11.6	132	2.1	465	53.5	18.7	99.7	115	80.9	250	140	99.2	43.7
DJF	99.6		14.8	116	2.1	862	120	38.1	29.5	29.7	130	106	31.7	5.6	3.5
MAM	128		20.8	149	2.1	83.4	11.9	3.5	7.7	15.1	32.4	123	64.0	6.1	3.8
JJA	94.5		3.5	97.6	1.6	160	33.2	10.8	70.2	93.1	58.6	189	154	205	87.6
SON	146		9.7	156	2.4	725	59.4	23.8	235	260	1051	484	251	134	59.7
2018	90.3	22.0	6.5	96.1	1.2	335	62.7	22.4	59.1	69.4	63.9	269	71.8	80.9	43.1
DJF	88.5		9.7	98.1	1.3	587	66.3	22.6	38.6	49.7	105	137	37.6	4.8	2.8
MAM	101		11.3	112	1.3	150	15.0	8.0	11.8	15.3	55.5	183	43.9	13.2	8.4
JJA	123		4.5	127	1.4	481	113	42.4	137	156	84.1	494	144	217	113
SON	48.3		3.0	50.3	0.9	236	52.7	14.8	31.7	38.9	32.2	176	39.2	38.4	21.8
2019	102	24.2	12.5	115	1.3	547	120	30.2	138	161	90.7	504	217	251	113
DJF	109		24.2	133	1.3	1124	152	38.6	27.0	18.4	62.0	583	47.4	7.1	5.5
MAM	79.0		15.1	94.1	1.2	127	19.8	5.6	10.7	17.0	49.2	209	135	6.5	4.0
JJA	169		9.2	178	1.6	530	181	47.8	265	306	107	707	250	812	366
SON	63.1		3.6	66.5	1.0	565	148	34.8	251	301	144	581	410	212	93.1
2020	197	32.6	16.3	214	1.6	919	175	54.7	242	172	179	808	188	644	502
DJF	85.9		14.5	101	1.5	1370	205	69.6	29.0	25.6	75.7	431	64.6	7.4	4.5
MAM	137		25.2	163	1.2	229	29.3	12.3	22.5	22.7	24.3	145	36.3	15.5	8.8
JJA	334		10.8	345	1.9	1292	299	86.2	659	415	473	2160	386	2350	1850
SON	202		13.7	216	2.1	963	188	58.8	226	207	129	424	260	47.5	24.0
Mean ±SD															
Annual	128±48.0	27.9±5.6	11.7±4.0	139±51.7	1.6±0.2	567±251	103±56.2	31.5±16.2	135±78.5	129±46.8	104±51.5	457±260	154±63.6	267±261	176±220
DJF	95.8±11.0		15.8±6.1	112±16.2	1.5±0.4	986±337	136±58.0	42.2±19.7	31.0±5.2	30.9±13.4	93.0±30.2	314±213	45.3±14.4	6.2±1.2	4.1±1.2
MAM	111±26.1		18.1±6.1	129±31.8	1.4±0.4	147±61.0	19.0±7.6	7.4±3.8	13.2±6.5	17.3±3.6	40.4±14.5	168±38.5	69.9±45.1	10.3±4.7	6.3±2.7
JJA	180±107		7.0±3.5	187±110	1.6±0.1	616±480	157±113	46.8±30.9	283±264	243±146	181±196	888±876	234±113	896±1010	604±839
SON	115±72.3		7.5±5.1	122±77.8	1.6±0.7	622±305	112±66.6	33.1±19.0	186±103	202±115	103±49.4	416±173	240±152	108±81.4	49.7±33.8
H-S	102±19.0		15.7±4.1	117±23.0	1.5±0.4	518±156	68.9±24.7	22.8±9.4	23.7±3.6	26.1±2.0	77.3±21.8	233±105	79±63	9.2±3.0	5.7±1.7
NH-S	152±75.0		7.6±3.3	163±86.0	1.7±0.5	622±374	152±111	41.4±25.3	258±160	246±108	148±115	703±472	235±96	555±530	360±445

Notations: H-S = Heating season NH-S = Non-heating season



Table 2: Estimated annual mean concentrations (eq. 1 – 7) of sea salt aerosol (SSA), mineral dust (MD), non-sea salt sulfate (nss-SO₄²⁻), organic matter (OM = OC × 2.2; Turpin and Lim, 2001), and elemental carbon (EC) at Zeppelin Observatory 2017 to 2020. Unit: ng m⁻³.

	SSA	MD	nss-SO₄²⁻	OM	EC
2017	730	559	381	265	11.6
2018	618	279	243	199	6.5
2019	697	477	283	225	12.5
2020	684	1136	349	434	16.3
Mean ± SD	682 ± 46.9	613 ± 368	314 ± 62.6	281 ± 106	12 ± 4.0



Table 3: Annual, heating season, and non-heating season contributions of BB and FF to eBC (PMF) and BC (FLEXPART). BB is denoted RWC in the heating season and WF in the non-heating season. Heating season and non-heating season contributions of levoglucosan are included. Zeppelin Observatory, 2017 to 2020. Unit: %.

	2017		2018		2019		2020		Mean ± SD	
	PMF	FLEXPART	PMF	FLEXPART	PMF	FLEXPART	PMF	FLEXPART	PMF	FLEXPART
Annual										
<i>eBC_{FF}/eBC</i>	71	54	68	47	73	53	67	50	70 ± 2.7	51 ± 3.1
<i>eBC_{BB}/eBC</i>	29	46	32	53	27	47	33	50	30 ± 2.7	49 ± 3.1
Heating season										
<i>eBC_{FF}/eBC</i>	73	59	67	51	73	58	70	57	71 ± 2.7	56 ± 3.6
<i>eBC_{RWC}/eBC</i>	27	41	33	49	27	42	30	43	29 ± 2.7	44 ± 3.6
Non-heating season										
<i>eBC_{FF}/eBC</i>	65	43	72	35	73	41	58	37	67 ± 6.7	39 ± 3.3
<i>eBC_{WF}/eBC</i>	35	57	28	65	27	59	42	63	33 ± 6.7	61 ± 3.3
Seasonal/Annual										
<i>eBC_{FF_H-S}/eBC_{FF}</i>	77	73	80	80	78	79	75	74	77 ± 1.8	77 ± 3.8
<i>eBC_{FF_NH-S}/eBC_{FF}</i>	23	27	20	20	22	21	25	26	23 ± 1.8	23 ± 3.8
<i>eBC_{RWC}/eBC_{BB}</i>	69	58	83	68	78	65	65	55	74 ± 8.2	62 ± 6.0
<i>eBC_{WF}/eBC_{BB}</i>	31	42	17	32	22	35	35	45	26 ± 8.2	38 ± 6.0
Seasonal/Annual										
<i>eBC_{FF_H-S}/eBC</i>	55	39	54	38	56	42	50	37	54 ± 2.8	39 ± 2.4
<i>eBC_{FF_NH-S}/eBC</i>	16	14	14	9	16	11	17	13	16 ± 1.2	12 ± 2.3
<i>eBC_{RWC}/eBC</i>	20	27	26	36	21	31	22	28	22 ± 2.7	30 ± 4.1
<i>eBC_{WF}/eBC</i>	8.9	20	5.4	17	6.1	16	12	22	8.0 ± 2.9	19 ± 2.8
Seasonal/Annual										
<i>Levo_{RWC}/Levo</i>	64		56		53		36		52 ± 12	
<i>Levo_{WF}/Levo</i>	36		44		47		64		48 ± 12	

Notation: eBC = equivalent black carbon; FF = fossil fuel; BB = biomass burning; H-S = Heating season; NH-S = Non-heating season; Levo = Levoglucosan; WF = Wildfire; RWC = Residential wood combustion; For simplicity we state eBC for both PMF and FLEXPART methods, while the correct is BC for FLEXPART.



Table 4: BB and FF fractions of BC (monthly weighted) obtained by different approaches (PMF, FLEXPART, and Radiocarbon;LHS) for non-heating-season and heating season. Means are based on identical time stamps (see Table S3).

Methodology	Annual		NH-season (JJASO)		H-season (NDJFMAM)	
	BC _{BB} /BC	BC _{FF} /BC	BC _{BB} /BC	BC _{FF} /BC	BC _{BB} /BC	BC _{FF} /BC
PMF	27 ± 14	73 ± 14	31 ± 11	69 ± 11	25 ± 16	75 ± 16
FLEXPART	45 ± 5	55 ± 5	48 ± 18	52 ± 18	42 ± 10	58 ± 10
Radiocarbon;LHS	61 ± 15	39 ± 15	67 ± 5	33 ± 5	57 ± 18	43 ± 18

Notation: For simplicity we state BC for all methods, while the correct is eBC for PMF, BC for FLEXPART, and EC for Radiocarbon;LHS.



Figure 1. The Zeppelin observatory located at the Zeppelin Mountain (472 m a.s.l.) close to the Ny-Ålesund settlement at Svalbard (78°54'0 N, 11°53'0 E) in: winter (left panel); summer (middle panel); The light-blue line on the map shows the Arctic Circle (66 °North) (right panel). (Foto: Ove Hermansen, NILU; Map: Finn Bjørklid, NILU).

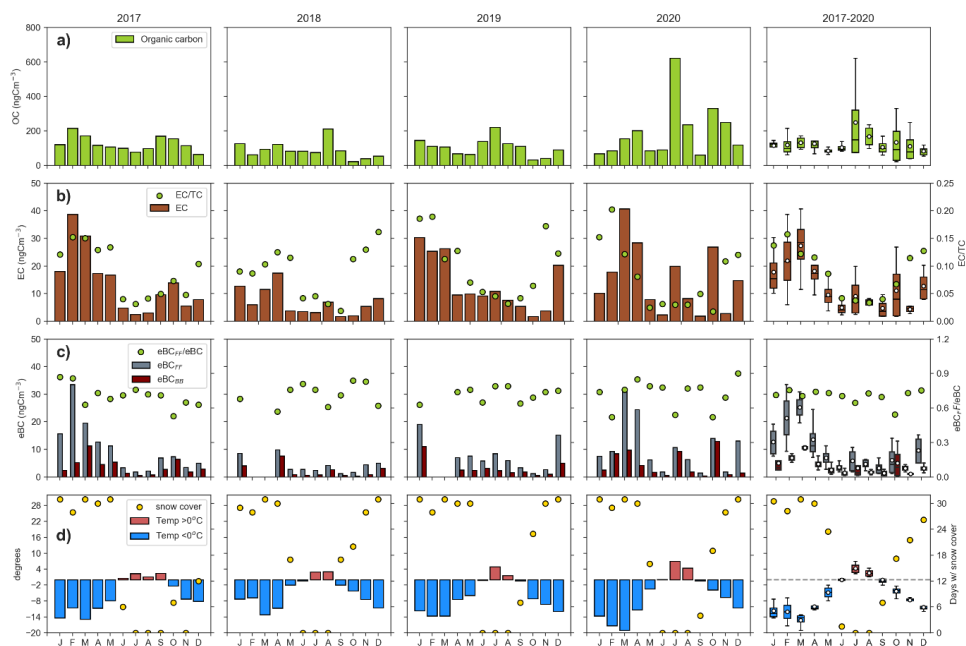


Figure 2. Panels show monthly mean concentrations for 2017 to 2020 and box plots (mean, 25, 50, 75 percentiles and IQR) for 2017 to 2020 at Zeppelin Observatory for a) OC; b) EC and EC/TC; c) eBC_{BB}, eBC_{FF}, and eBC_{FF}/eBC; d) Ambient temperature and days with snow on ground. Concentrations in a) - c) are measured in the PM₁₀ size fraction.

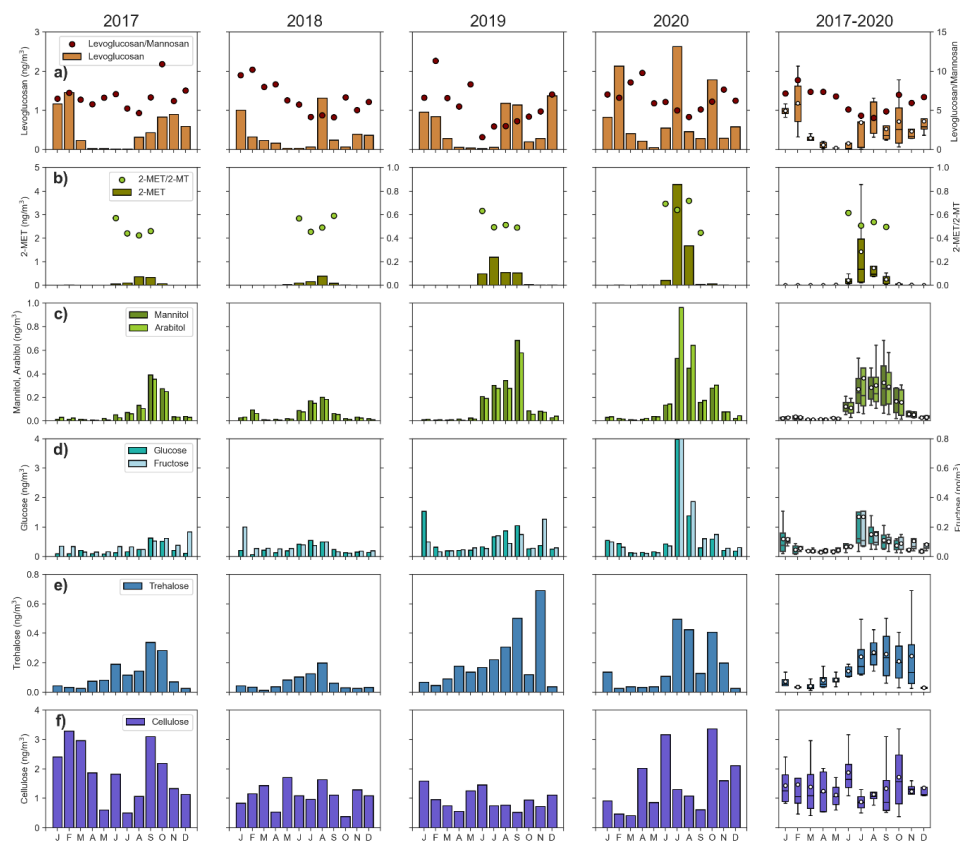


Figure 3. Panels show monthly mean concentrations for 2017 to 2020 and box plots (mean, 25, 50, 75 percentiles and IQR) for 2017 to 2020 at Zeppelin Observatory for a) Levoglucosan and levoglucosan/mannosan; b) 2-methylerythritol (2-MET), 2-methylthreitol (2-MT), and 2-MT)/2-MET; c) Mannitol, arabitol, and mannitol/arabitol; d) Fructose and glucose; e) Trehalose; f) Cellulose. All variables are measured in the PM₁₀ size fraction.

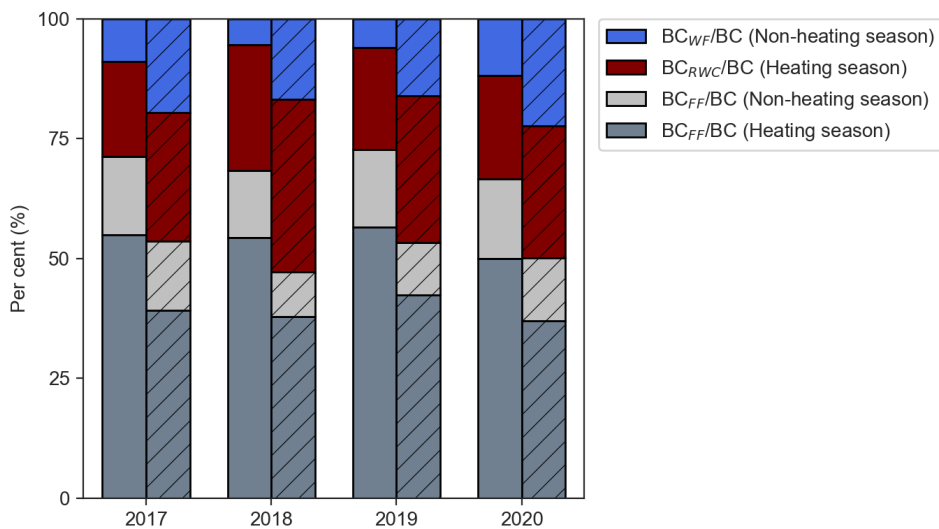


Figure 4. eBC (PMF) (without diagonal lines) and BC (FLEXPART) (with diagonal lines) apportioned to biomass burning (BB) and fossil (FF) fuel combustion according to heating season and non-heating season. BB is denoted wildfire (WF) in summer and residential wood combustion (RWC) in winter. Zeppelin Observatory (2017 to 2020). For simplicity we state BC for all methods, while the correct is eBC for PMF, BC for FLEXPART.

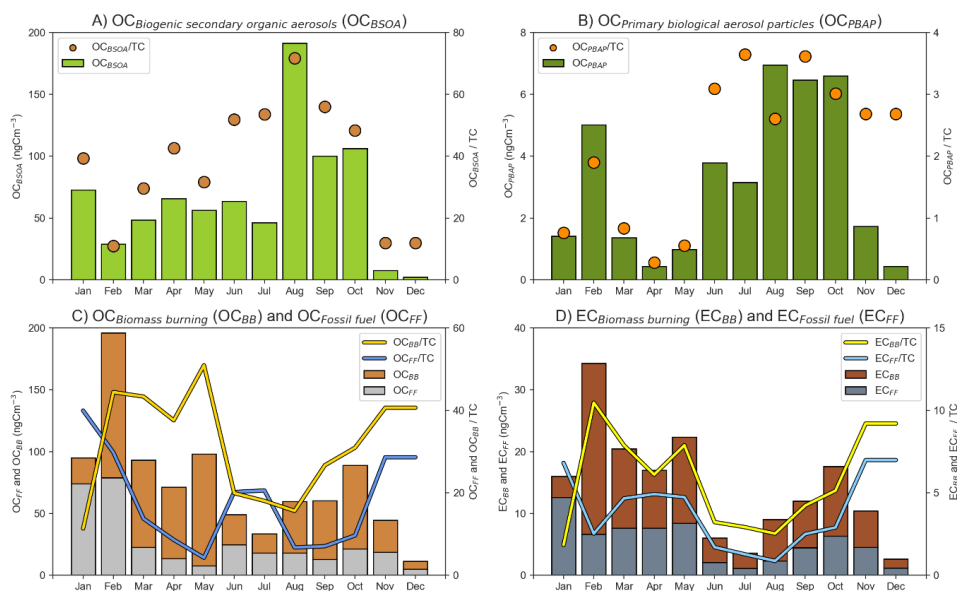


Figure 5. Panels show monthly mean concentrations and relative contributions for samples collected in 2017 to 2018 at Zeppelin Observatory for A) Biogenic Secondary Organic Aerosol (OC_{BSOA}) and OC_{BSOA}/TC; B) Primary Biological Aerosol Particles (OC_{PBAP}), being the sum of fungal spores (OC_{PBS}) and plant debris (OC_{PBC}), and OC_{PBAP}/TC; C) Biomass burning (OC_{BB}, OC_{BB}/TC) and fossil fuel sources (OC_{FF}, OC_{FF}/TC; D) Fossil fuel (EC_{FF}, EC_{FF}/TC) and biomass burning (EC_{BB}, EC_{BB}/TC), source apportioned using the LHS approach (Sect. 2.7).

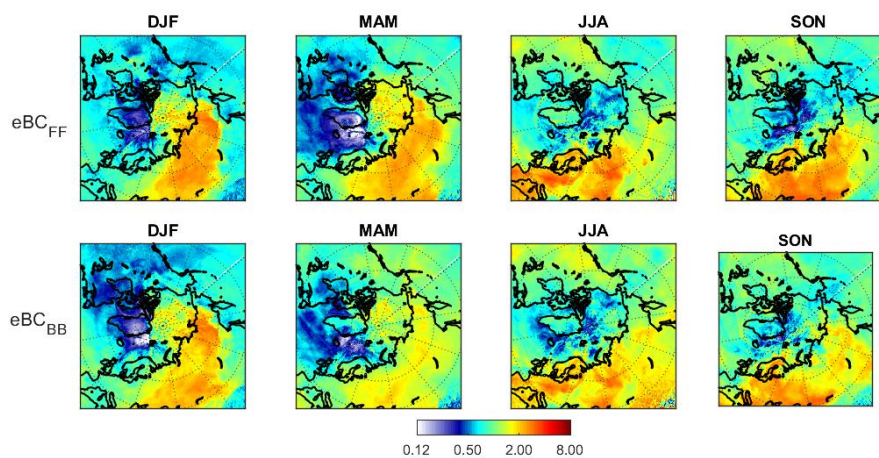


Figure 6. Ratio between footprints for the 80 percentiles of eBC_{FF} (upper panels) and eBC_{BB} (lower panels) and all footprints for this season. Seasons are split into December, January, and February (DJF), March, April, and May (MAM), June, July, and August (JJA), and September, October, and November (SON). High values (red) colors indicate source regions which lead to high concentrations at the receptor site Zeppelin. Average seasonal footprints of the highest (80 percentile) eBC_{BB} and eBC_{FF} concentrations observed at Zeppelin relative to the average footprint.

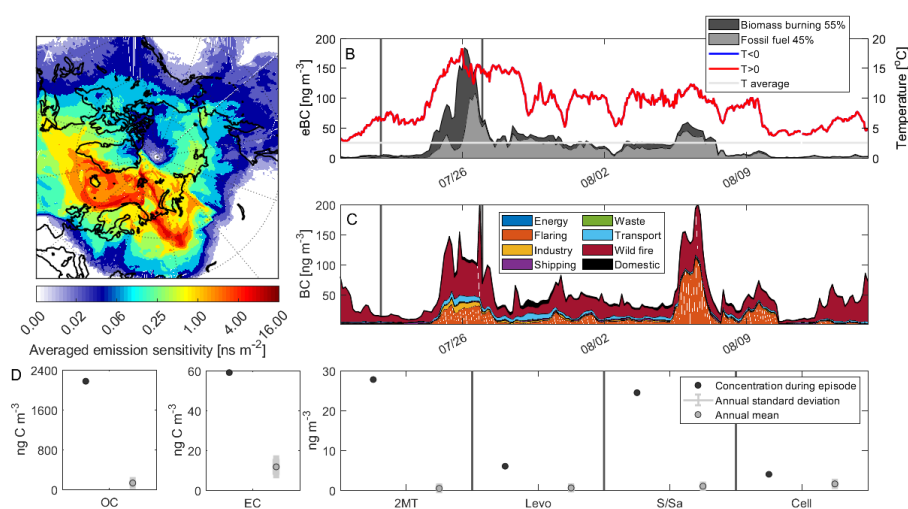


Figure 7. LRT episode at Zeppelin Observatory covered by filter sample collected 22 – 27.07.2020. A) Averaged footprint sensitivity for sample collected 22 – 27.07.2020; B) Hourly time series of eBC_{BB} and eBC_{FF} (PMF) and ambient temperature. The period covered by the filter sample is defined by the dark grey vertical lines; C) Hourly time series of modelled BC concentrations from different source categories; D) Concentrations of OC, EC, and organic tracers (2MT = 2-Methyltetrols; Levo = Levoglucosan; S and SA = Sugars and Sugar-alcohols; Cell = Cellulose) obtained for the filter sample compared to the long-term annual mean and its standard deviation.

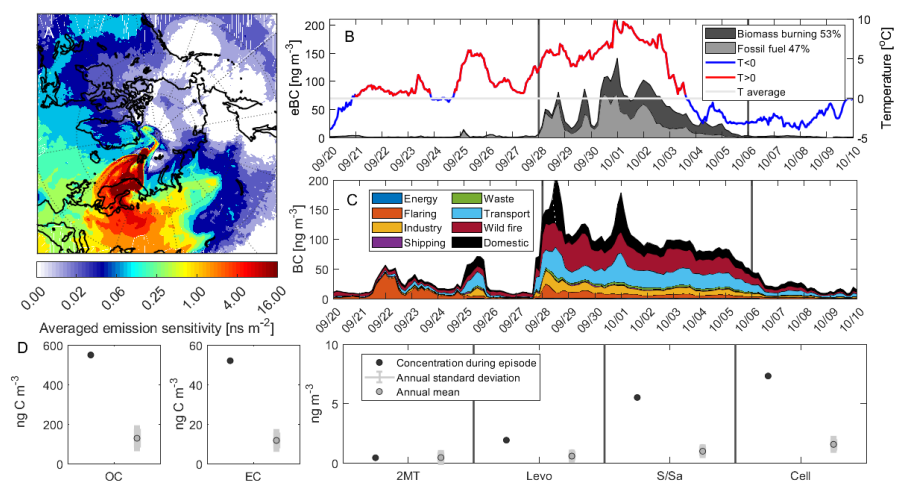


Figure 8. Same as Fig. 7, but for 28.09 – 06.10.2017.

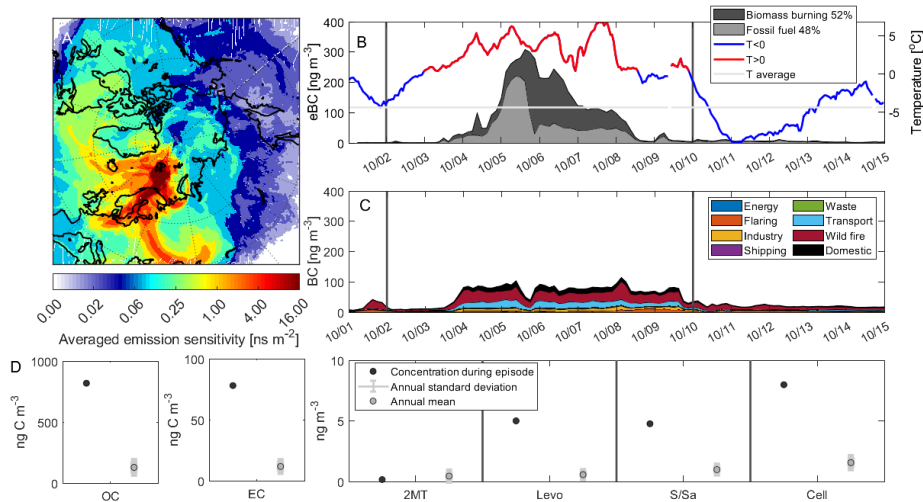


Figure 9. Same as Fig. 7, but for 2 – 10.10.2020.